Inflammatory Bowel Diseases

The inflammatory bowel disease drug azathioprine induces autophagy via mTORC1 and the unfolded protein response sensor PERK

--Manuscript Draft--

Manuscript Number:	IBD-D-18-00939R1
Article Type:	Original Research Articles - Basic Science
Keywords:	Azathioprine; autophagy; mTORC1; unfolded protein response; Adherent-invasive E.coli.
Corresponding Author:	Craig Stevens, PhD Edinburgh Napier University Faculty of Health Life and Social Sciences Edinburgh, United Kingdom
First Author:	Kirsty M. Hooper, PhD
Order of Authors:	Kirsty M. Hooper, PhD
	Victor Casanova, PhD
	Sadie Kemp, BSc
	Katherine A. Staines, PhD
	Jack Satsangi, FRSE
	Peter G. Barlow, PhD
	Paul Henderson, MBChB, PhD
	Craig Stevens, PhD
Manuscript Region of Origin:	UNITED KINGDOM
Abstract:	Background Genetic studies have strongly linked autophagy to Crohn's disease (CD) and stimulating autophagy in CD patients may be therapeutically beneficial. The aim of this study was to evaluate the effect of current inflammatory bowel disease (IBD) drugs on autophagy and investigate molecular mechanisms of action and functional outcomes in relation to this cellular process. Methods Autophagy marker LC3 was evaluated by confocal fluorescence microscopy and flow cytometry. Drug mechanism of action was investigated by PCR Array with changes in signaling pathways examined by immunoblot and RT-qPCR. Clearance of adherent-invasive Escherichia coli (AIEC) and levels of pro-inflammatory cytokine tumour necrosis factor alpha (TNFα) were evaluated by gentamicin protection assays and RT-qPCR respectively. LC3 was analysed in peripheral blood mononuclear cells (PBMC) from paediatric patients by flow cytometry. Results Azathioprine induces autophagy via mechanisms involving modulation of mechanistic target of rapamycin (mTORC1) signaling and stimulation of the unfolded protein response (UPR) sensor PERK. Induction of autophagy with azathioprine correlated with the enhanced clearance of AIEC and dampened AIEC-induced increases in TNFα. Azathioprine induced significant increase in autophagosome bound LC3-II in PBMC populations ex vivo, supporting in vitro findings. In patients, the CD-associated ATG16L1 T300A single-nucleotide polymorphism did not attenuate azathioprine induction of autophagy. Conclusions Modulation of autophagy via mTORC1 and the UPR may contribute to the therapeutic

	efficacy of azathioprine in IBD.

The inflammatory bowel disease drug azathioprine induces autophagy via mTORC1 and the unfolded protein response sensor PERK

Kirsty M. Hooper, PhD[1], Victor Casanova, PhD[1], Sadie Kemp, BSc[1], Katherine A. Staines, PhD[1], Jack Satsangi, FRSE[2,5], Peter G. Barlow, PhD[1], Paul Henderson, MBChB, PhD[3, 4¶] and Craig Stevens, PhD[1¶*].

1. School of Applied Sciences, Edinburgh Napier University, Sighthill Campus, Sighthill Court, Edinburgh, EH11 4BN.

2. Centre for Genomic & Experimental Medicine, University of Edinburgh, Western General Hospital Campus, Crewe Road, Edinburgh EH4 2XU.

3. Child Life and Health, University of Edinburgh, Edinburgh, EH9 1UW.

4. Department of Pediatric Gastroenterology and Nutrition, Royal Hospital for Sick Children, Edinburgh, EH9 1LF.

5. Translational Gastroenterology Unit, Nuffield Department of Medicine, John Radcliffe Hospital, Oxford OX3 9DU.

¶Joint senior authors

Short title: The CD drug azathioprine induces autophagy

Address for correspondence

*Dr Craig Stevens

School of Applied Sciences, Edinburgh Napier University, Sighthill Campus, Sighthill Court, Edinburgh, EH11 4BN.

Email: C.Stevens@napier.ac.uk

Tel: 0044 131 455 2930

Summary

The aim of this study was to evaluate the effect of current inflammatory bowel disease drugs on autophagy and investigate molecular mechanisms of action and functional outcomes in relation to this cellular process.

Abstract

Background: Genetic studies have strongly linked autophagy to Crohn's disease (CD) and stimulating autophagy in CD patients may be therapeutically beneficial. The aim of this study was to evaluate the effect of current inflammatory bowel disease (IBD) drugs on autophagy and investigate molecular mechanisms of action and functional outcomes in relation to this cellular process.

Methods: Autophagy marker LC3 was evaluated by confocal fluorescence microscopy and flow cytometry. Drug mechanism of action was investigated by PCR Array with changes in signaling pathways examined by immunoblot and RT-qPCR. Clearance of adherent-invasive *Escherichia coli* (AIEC) and levels of pro-inflammatory cytokine tumour necrosis factor alpha (TNFα) were evaluated by gentamicin protection assays and RT-qPCR respectively. LC3 was analysed in peripheral blood mononuclear cells (PBMC) from pediatric patients by flow cytometry.

Results: Azathioprine induces autophagy via mechanisms involving modulation of mechanistic target of rapamycin (mTORC1) signaling and stimulation of the unfolded protein response (UPR) sensor PERK. Induction of autophagy with azathioprine correlated with the enhanced clearance of AIEC and dampened AIEC-induced increases in TNFα. Azathioprine induced significant increase in autophagosome bound LC3-II in PBMC populations *ex vivo,* supporting *in vitro* findings. In patients, the CD-associated *ATG16L1 T300A* single-nucleotide polymorphism did not attenuate azathioprine induction of autophagy.

Conclusions: Modulation of autophagy via mTORC1 and the UPR may contribute to the therapeutic efficacy of azathioprine in IBD.

Keywords: Azathioprine, autophagy, mTORC1, unfolded protein response, Adherent-invasive *E.coli*.

Introduction

The inflammatory bowel diseases (IBD), Crohn's disease (CD), ulcerative colitis (UC) and IBD-unclassified (IBDU), are characterized by chronic inflammation of the gastrointestinal (GI) tract and have a prevalence of up to 400 per 100,000 people in the United Kingdom [1]. The pathogenesis of IBD is multifactorial in nature, with genetic predisposition, breakdown of the intestinal epithelial barrier, and concomitant interaction with environmental triggers in the lumen contributing to disease[2]. A dysregulated immune response to intestinal microflora has been heavily implicated, and examination of the disease-associated microbiome has identified several potentially causative agents [3]. Most notably *Escherichia coli* (*E.coli)* strains with an adherent and invasive phenotype (AIEC) have been consistently isolated by independent investigators from CD patients with ileal disease [4].

Genome-wide association studies (GWAS) have identified 240 IBD susceptibility loci to date[5] and have confirmed association with previously recognized susceptibility genes including *Nucleotide-binding oligomerisation domain-containing protein 2 (NOD2)*. Amongst genes identified are several linked to autophagy including *autophagy-related protein* (*ATG*)*16L1, Immunity-related GTPase family M protein* (*IRGM*) and *leucine rich repeat kinase 2* (*LRRK2*) [6]. Autophagy is an intracellular homeostatic process that involves the formation and maturation of double membrane vesicles, known as autophagosomes, which engulf cargo that is degraded upon fusion with lysosomes [7]. Autophagy can be an important survival mechanism that is induced in response to a myriad of stresses. Autophagy plays an essential role in the innate and adaptive immune responses and the timely resolution of inflammation [8], and loss of immune regulation is a key event leading to the chronic inflammation observed in CD [9]. Notably, impaired autophagy responses have been observed in a range of cell types derived

from CD patients including the specialized intestinal epithelial cells (IECs) Paneth cells and goblet cells, and leukocytes, such as macrophages and dendritic cells (DC) [10].

Evidence suggests that inducing autophagy may have therapeutic benefit for the treatment of IBD [9]. Mechanistic target of rapamycin complex 1 (mTORC1) is a master regulator of cell growth and a potent inhibitor of autophagy [10], therefore inhibition of mTORC1 with rapamycin or its analogues, sirolimus and everolimus, strongly induces autophagy. In previously reported case studies sirolimus improved symptoms and intestinal healing in a patient with severe refractory CD [11] and everolimus controlled symptoms for 18 months in a patient with refractory UC [12]. In a study of refractory pediatric IBD, sirolimus induced clinical remission in 45% of UC patients and 100% of CD patients [13].

Drugs currently approved for clinical use for IBD, including corticosteroids, immunomodulators, aminosalicylates (5-ASAs) and biologics, target the immune system to reduce inflammation and induce remission, however response to treatment often diminishes over time, with 10–35% of CD patients requiring surgery within a year of diagnosis and up to 61% by 10 years [14]. A National Health Service review estimated IBD treatment costs of £720 million ($940m) per year in the United Kingdom alone [1], with roughly a quarter of these costs directly attributed to drug treatments [15]. The Crohn's and Colitis Foundation has recently highlighted the need for research into optimizing existing medical therapies [16], with patient stratification of key importance in this context [13]. In order to optimize therapies, a more comprehensive understanding of drug mechanisms of action is required.

We aimed to evaluate current IBD drugs in the context of autophagy and show that the immunomodulator azathioprine induces autophagy via mechanisms involving modulation of

mTORC1 and stimulation of the unfolded protein response (UPR) sensor PERK. Our results suggest that in addition to well-characterized effects on DNA/RNA synthesis and T-lymphocytes [17,18], modulation of autophagy and the UPR may contribute to the therapeutic efficacy of azathioprine.

Materials and Methods

Cell culture, transfection, plasmids and reagents

HEK293 cells were grown in Dulbecco's modified Eagle medium (DMEM) (Gibco, ThermoFisher Scientific, Paisley, UK) supplemented with 10% foetal bovine serum (FBS) (Invitrogen, ThermoFisher Scientific) and penicillin streptomycin (Gibco). The monocytic THP-1 cell line was grown in RPMI 1640 (Sigma-Aldrich, Irvine, UK), supplemented with 10% FBS, penicillin streptomycin and 200mM L-glutamine (Gibco). For differentiation to macrophages, THP-1 cells were incubated in RPMI growth media supplemented with 10ng/ml phorbol myristate acetate (PMA) (Sigma-Aldrich, Dorset, UK) for 48 hr, then rested for 24 hr in fresh RPMI growth media prior to experiments.

For transfection of HEK293 cells, a Nucleofector Kit V (Lonza Ltd, Manchester, UK) was used according to the manufacturer's instructions. The GFP-LC3 [19], GFP-RFP-LC3 [20] and x-light EGFP [21] plasmids have been described previously. All reagents used are detailed in supplementary (Table S1). For nutrient deprivation, cells were incubated with Earle's Balanced Salt Solution (EBSS) (Gibco).

Immunoblotting

Cells were lysed in ice-cold extraction buffer (50mM Tris [pH 7.6], 150mM NaCl, 5mM EDTA, 0.5% NP-40, 5mM NaF, 1mM sodium vanadate, 1 × Pierce Protease Inhibitor Cocktail [Thermo Scientific]) for 30 min followed by centrifugation. Protein lysates were resolved by denaturing electrophoresis on acrylamide/bisacrylamide gels and electro-transferred to Immobilon-FL PVDF membrane (Merck Millpore EMD, Watford, UK). Membranes were incubated with

primary antibodies overnight at 4°C, and after washing, were incubated with a secondary antibody for 1hr at room temperature (RT). Antibody details are provided in (Table S2). Proteins were visualized by incubation with an ECL western blotting analysis system (GE Healthcare) and imaged using a G: BOX system (Syngene, Cambridge, UK). Relative intensity of bands were measured using Image J software [22] (National Institutes of Health, Bethesda, MD, USA).

Confocal fluorescence microscopy

Cells were seeded on 21-mm borosilicate glass cover slips, 8 chamber polystyrene vessel CultureSlides (Falcon, Fisher Scientific, Loughborough, UK) or 35mm imaging dishes (Ibidi, Thistle Scientific, Uddingston, UK). Images were captured using Carl Zeiss LSM880 confocal microscope (Jena, Germany) and images were analysed using Image J software [18] (National Institutes of Health).

For fixed cell imaging: Cells were fixed with 4% paraformaldehyde (PFA) for 15 min, permeabilized with PBS/0.2% Triton X-100 (Sigma Aldrich) and blocked with PBS containing 10% goat's serum (Gibco) and 2.5% Human TruStain FcX (BioLegend, San Diego, USA). Primary antibodies (Table S2) were incubated overnight at 4°C and conjugated secondary antibodies for 1hr at RT. Where appropriate, cells were counterstained with 4',6'-diamidino-2-phenylindole (DAPI) or mounted with Vectashield mounting medium for fluorescence with DAPI (Vector Laboratories, Peterborough, UK).

For live cell imaging: Cells were grown in 35mm imaging dishes (Ibidi) and maintained at 37^{o}C and 5% CO_2 in live-cell imaging chamber attached to Carl Zeiss LSM880 confocal microscope. Images were captured every 2 minutes at x40 magnification over a 12hr time period.

For autophagy assays in HEK293 GFP-LC3 stable cells: The basal threshold number of GFP-LC3 puncta per cell was established as 5, and cells exhibiting ≥5 puncta were regarded as having enhanced autophagy activity.

For tandem fluorescent-tagged GFP-RFP-LC3 assays: Cells were transiently transfected with the GFP-RFP-LC3 plasmid and following designated treatments, the fluorescent autophagy markers GFP-RFP-LC3 or RFP-LC3 were observed using a confocal microscope and the number of (RFP+GFP+) and (RFP+GFP-) puncta per cell determined.

Flow cytometry

Peripheral blood mononuclear cells (PBMC) were seeded in 96-well U-bottom plates and cell lines were seeded in 12-well plates. After treatments, cells were gently detached using 0.05% trypsin or Cell Dissociation Solution Non-enzymatic (Sigma Aldrich) at 37°C for 10 min. Cells were acquired using the BD Biosciences (Oxford, UK) Celesta flow cytometer or the FACSCalibur (BD) and data analysis performed using BD FACsDiva Software or FlowJo software.

Autophagy assay: For HEK293 GFP-LC3, cells were collected then washed in 0.05% w/v saponin (Sigma), diluted in PBS to remove the unbound cytosolic LC3 [23], which does not alter expression of membrane antigens [24], prior to acquisition. For PBMC, cells were collected and blocked with 2.5% Human TruStain FcX in PBS for 20 min, then incubated with PBMC surface markers or IgG isotypes diluted in Brilliant Stain Buffer (BD Horizon) for 25 min, both at RT. Cells were then washed in 0.05% w/v saponin, diluted in PBS to remove the unbound cytosolic LC3, and fixed with 1% PFA for 20 min at 4^{o}C. Cells were washed again with 10% goat serum in 0.05% saponin before overnight incubation with primary LC3 antibody or Rb IgG Isotype

control (Invitrogen) in 1% goat serum in 0.05% saponin at 4°C. Secondary antibody in 1% goat serum in 0.05% saponin was incubated for 30 min at 4°C prior to washing and acquisition.

Annexin-V/PI assay. Cells were stained using the FITC Annexin V Apoptosis Detection Kit I (BD Pharmingen) according to manufacturer's instructions.

RT-qPCR

Cells were scraped into RNAzol RT (Sigma-Aldrich) and total RNA extracted according to manufacturer's instructions. Total RNA was quantified using a NanoDrop 2000 Spectrophotometer (Thermo Scientific) and integrity was assessed using an Agilent 2100 Bioanalyzer (Agilent Technologies, Stockport, UK) with RNA Nano Chips and Agilent RNA 6000 Nano Reagents (Agilent Technologies). mRNA was converted to cDNA using nanoScript 2, Reverse Transcription Premix (PrimerDesign Ltd, Chandler´s Ford, UK) according to manufacturer's instructions. For qPCR analysis of gene expression PrecisionPLUS Mastermix with SYBR green and ROX with inert blue dye (PrimerDesign) was used according to manufacturer's instructions with RT-PCR Grade Water (Invitrogen) and the StepOnePlus Real-time PCR System (Applied Biosystems, ThermoFisher). Primers are detailed in supplementary (Table S3). A geNorm kit (PrimerDesign) was used for the selection of appropriate reference genes (*RPL13A* [*Ribosomal Protein L13a*] and *Actin*) with the qbase+ software [25]. 2^{-ddCT} was used for relative quantification of gene expression [26]. The RT² Profiler PCR Array of Human Autophagy genes (Qiagen, Crawley, UK) was performed according to manufacturer instructions.

Bacterial infection assays

For growth curves: LB was inoculated with *E. coli* strain CUICD541-10 [27] isolated from the ileum of a patient with CD (a kind gift from Prof Kenny Simpson, Cornell University, USA), from an overnight culture to an optical density of 0.05 at 600nM. Cultures were treated appropriately, incubated at 37^{o}C with 200rpm shaking, and optical density was measured at 600nM every 30 min.

For intracellular survival: Cells were infected with CUICD541-10 *E. coli* at a multiplicity of infection (MOI) of 10 for 3hr, incubated for 1hr in 100µg/ml gentamicin (Gibco) to kill extracellular bacteria, then maintained for a further 24hr in 20µg/ml gentamicin, with addition of appropriate treatments for the final 6hr. For colony forming unit (CFU) enumeration, cells were lysed for 10 min using 1% Triton X100 in PBS. Lysates were serially diluted and plated on LB agar plates for overnight incubation at 37°C.

For immunofluorescence: CUICD541-10 *E. coli* transformed with an x-light mCherry plasmid were used and 30 min prior to immunostaining cells were incubated with 0.1mM isopropyl β-D-1-thiogalactopyranosid (IPTG) (Sigma) to promote bacterial fluorescence. IPTG and 5µM Cell Tracker Green BODIPY (Invitrogen) were added for the duration of the live-cell imaging of infected cells.

Patients

Patient recruitment and sample collection was performed at the Royal Hospital for Sick Children in Edinburgh, and processing and analysis was performed at Edinburgh Napier University.

Inclusion criteria were: (1) aged 6-18 years on date of colonoscopy; (2) already confirmed CD, UC or IBDU [28] or undergoing first upper and lower GI endoscopy due to gastrointestinal symptoms suggestive of possible bowel inflammation (e.g. abdominal pain, peri-rectal (PR) bleeding, weight loss). Non-IBD patients were defined as those with both microscopically and macroscopically normal colonoscopy. Patients were excluded if they had previously undergone colonoscopy for anything other than known IBD, were diagnosed with anything other than IBD following a full investigative cycle, or who could not provide written consent. Whole blood samples (maximum 15ml), and saliva samples were collected from patients: 20 IBD cases and 9 non-IBD controls (Table S4). PBMC were isolated from whole blood using Ficoll-Paque PLUS (GE Healthcare Bio-Sciences AB, Uppsala, Sweden) and cultured in RPMI growth media. Saliva samples were collected using Oragene DNA kits (DNA Genotek, Ontario, Canada).

Genotyping

Saliva samples were sent to the Wellcome Trust Clinical Research Facility in Edinburgh for analysis. Once recruitment was completed, DNA was extracted using Isohelix kit and Taqman genotyping for each sample was performed for the following SNPs: *ATG16L1 T300A* (rs2241880), *NOD2 L1007f/s* (p.Leu1007fsX1008) (rs2066847), *NOD2 R702W* (rs2066844) and *NOD2 G908R* (rs2066845).

Statistical analysis

Results are reported as the mean ± SEM assuming normally distributed variables with statistical analysis conducted by using one-way or two-way ANOVA, or paired t-test as appropriate, with GraphPad Prism version 7.0 (GraphPad Software, CA, USA).

Ethics

All samples were collected with local institutional and NHS ethical approvals (reference 16/WW/0210). Eligible patients were approached at least 48hr prior to colonoscopy and following consent were recruited to the study.

Data availability

The datasets generated during and/or analysed during the current study are available from the corresponding author on reasonable request.

Results

Azathioprine induces autophagosome accumulation

To evaluate the modulation of autophagy by IBD drugs we used HEK293 cells, a well-characterized cell line used in autophagy research [29] that were engineered to stably express the autophagy marker LC3 fused to green fluorescent protein (GFP-LC3) [30]. GFP-LC3 puncta accumulation was measured by live-cell imaging (Figure 1A). Significant increases in GFP-LC3 puncta number were observed after treatment with the immunomodulator azathioprine (Figure 1A, panel iv and ix) and the biologic infliximab (Figure 1A, panel v and ix) with an optimal time-point of 6 hr for both drugs (Figure 1A, panel x and xi). Significant increases in GFP-LC3 puncta were also observed with EBSS to induce nutrient deprivation, a strong activator of the autophagy pathway (Figure 1A, panel iii and ix). In contrast, the immunomodulator methotrexate (Figure 1A, panel vi, ix and xii), the corticosteroid methylprednisolone (Figure 1A, panel vii, ix and xiii) and the aminosalicylate sulfasalazine (Figure 1A, panel viii, ix and xiv) had no significant effects on GFP-LC3 puncta accumulation.

Azathioprine activates the autophagy pathway

Autophagosomes can accumulate due to activation or inhibition of the autophagy pathway. To distinguish between these processes, we first employed flow cytometric analysis. To facilitate measurement of autophagy activation by flow cytometry, HEK293 GFP-LC3 cells were washed with the glycoside saponin to permeabilize cell plasma membranes prior to analysis. Plasma membrane permeabilization releases inactive cytosolic LC3, with only the active lipidated form of LC3-II, which is tightly associated with autophagosome membranes,

being retained [23] (Supplementary Figure 1). Additionally, Bafilomycin A1 (BafA1), an inhibitor of autophagosome-lysosome fusion[30], was used to augment LC3-II accumulation. Under these conditions azathioprine clearly enhanced the accumulation of autophagosome-bound GFP-LC3-II (Figure 2A, panel ii and quantified in iv). In contrast, infliximab had only minor additional effect on GFP-LC3-II accumulation (Figure 2A, panel iii and iv).

To further validate that azathioprine-mediated activation of the autophagy pathway, we employed a tandem RFP-GFP-LC3 plasmid [31]. This RFP-GFP-LC3 plasmid utilises the pH difference between the acidic autolysosome (formed by fusion of an autophagosome and lysosome) and the neutral autophagosome, with the pH sensitivity differences exhibited by GFP (labile at acidic pH) and RFP (stable at acidic pH). Thus, this plasmid can be used to monitor progression from the autophagosome (RFP+GFP+) to the autolysosome (RFP+GFP-). HEK293 cells were transfected with RFP-GFP-LC3 plasmid and treated with BafA1, EBSS or azathioprine. As expected, all three treatments caused autophagosomes to accumulate (Figure 2B, panel xvi). Inhibition of autophagosome-lysosome fusion with BafA1 resulted in the accumulation of (RFP+GFP+) puncta, which appear as yellow in the merged image (Figure 2B, panel x, xiii and quantified in xvii), while activation of the pathway with EBSS resulted in an accumulation of (RFP+GFP-) puncta indicating that complete progression through the pathway was taking place (Figure 2B, panel xi, xiv and xvii). Azathioprine treatment resulted in an accumulation of (RFP+GFP-) puncta relative to untreated control (Figure 2B, panel xii, xv and xvii) indicating that azathioprine activates the autophagy pathway.

Azathioprine induces autophagosome accumulation in macrophages independent of apoptosis

As with other biological processes, autophagy is cell-type specific and it is therefore essential to determine how azathioprine modulates the autophagy pathway in cell types of direct relevance to IBD. For this purpose, macrophages derived from THP-1 cells were treated with azathioprine and endogenous LC3 puncta accumulation measured by fixed-cell confocal fluorescence microscopy. In line with our previous results (Figure 1A), azathioprine treatment significantly increased the number of LC3 puncta in THP-1 derived macrophages (Figure 3A, panel iv and v). Autophagy and apoptosis are intimately linked [32], therefore it was also important to determine the effect of azathioprine on apoptosis in these cells. Analysis of Annexin V/PI staining by flow cytometry revealed that azathioprine had no effect on cell viability at either 6 hr or 24 hr treatment (Figure 3B, panel ii, iv, and v). Together, these results demonstrate that azathioprine induces autophagosome accumulation in THP-1 derived macrophages independent of apoptosis.

Azathioprine stimulates the UPR

To gain insight into azathioprine mechanism of action, we used the Human Autophagy RT² Profiler PCR Array. Gene expression was compared in THP-1 derived macrophages either left untreated or treated with azathioprine (Figure S3). Among the genes significantly up-regulated by azathioprine was the UPR-regulating kinase EIF2AK3 (also known as PERK). As endoplasmic reticulum (ER)-stress/UPR genes are strongly associated with IBD this was investigated further [33]. A time-course RT-qPCR experiment identified 6 hr as the optimum time-point for up regulation of PERK, which occurred in a dose-dependent manner (Figure 4, panel i and ii). The expression of genes downstream from PERK (ATF4, and CHOP; Figure 4, panel iii and iv), and the ER stress chaperon protein disulphide isomerase (PDI) (Figure 4, panel

vi) were also up regulated after 6 hr of azathioprine treatment in a dose dependent manner. In contrast, expression of the ER stress chaperone protein binding immunoglobulin protein/78-kDa glucose-regulated protein (BiP/Grp78) was not affected by azathioprine treatment after 6 hr (Figure 4, panel vii) however a minor increase was observed after 24 hr. These results indicate that azathioprine stimulates the UPR.

Azathioprine modulates mTORC1 signaling

mTORC1 is a major regulatory hub balancing cell growth and protein translation with control of autophagy [34]. When active, mTORC1 is a potent inhibitor of autophagy. Therefore, levels of phosphorylated ribosomal protein S6 (p-rpS6), a surrogate marker of mTORC1 activity, were evaluated in THP-1 derived macrophages treated with increasing concentrations of azathioprine. Azathioprine treatment caused a dramatic decrease in p-rpS6 in a dose dependent manner (Figure 5A, lanes 3-6 and quantified in ii). These results suggest that azathioprine treatment inhibits mTORC1 activity.

Azathioprine modulates mTORC1 signaling independent of PERK

PERK has been shown to inhibit mTORC1 in response to ER stress as part of a mechanism to induce autophagy [34–36]. To test whether modulation of mTORC1 observed in response to azathioprine is dependent on PERK, THP-1 derived macrophages were treated in the absence or presence of a pharmacologic inhibitor of PERK. Azathioprine again caused a decrease in p-rpS6, and the PERK inhibitor did not significantly alter this effect (Figure 5B, panel i, compare lanes 3 and 8, and quantified in ii). To confirm PERK inhibitor activity, phosphorylation of eIF2a, a well-characterized substrate of PERK, was assessed (Figure 5B, lanes 6-10 and

quantified in iii). These results suggest that modulation of mTORC1 signaling by azathioprine occurs independent of PERK.

Azathioprine-induced autophagy is modulated by PERK

To determine whether PERK is required for azathioprine-induced autophagy, THP-1 derived macrophages were treated with azathioprine or EBSS in the absence or presence of PERK inhibitor. In the presence of PERK inhibitor, azathioprine-induced autophagy was specifically attenuated (Figure 5C, compare panel ii and v, and quantified in vii) compared to EBSS-induced autophagy (Figure 5C, compare panel iii and vi, and quantified in vii). These results indicate that PERK is an important factor regulating azathioprine-induced autophagy.

Azathioprine enhances clearance of intracellular *AIEC*

Evidence suggests that AIEC play a putative role in CD [37]. Therefore, we evaluated the survival of the CD mucosa-associated AIEC strain CUICD541-10 [27] in THP-1 derived macrophages. Initially, it was determined that azathioprine had no direct effect on bacterial growth (Figure S3). Azathioprine treatment did however cause a significant decrease in bacterial CFU in AIEC infected cells (Figure 6A). Furthermore, immunofluorescence analysis showed a decrease in the percentage of cells infected with bacteria (Figure 6B and C, compare panels iii and iv and quantified in v), which correlated with an increased accumulation of LC3 puncta (Figure 6C panel v) indicating that autophagy was being induced.

Infection of cells with AIEC elicits a strong inflammatory response; therefore, RT-qPCR was used to assess expression of the pro-inflammatory cytokine TNFα in THP-1 derived macrophages infected with AIEC. Expression was significantly up regulated by AIEC infection

and this was reduced when cells were treated with azathioprine (Figure 6D, panel i). Azathioprine also reduced the expression of TNFα in cells treated with bacterial lipopolysaccharide (LPS) (Figure 6D, panel ii) suggesting that azathioprine may affect TNFα expression independent of decreased intracellular bacteria. These results demonstrate that azathioprine enhances the clearance of intracellular AIEC and dampens the elevated cytokine levels observed in response to infection.

Azathioprine activates autophagy in PBMC and monocytes from pediatric patients

Non-IBD, CD and UC patients were genotyped for the CD-associated NOD2 (R702W, G908R, L1007fs) and *ATG16L1 T300A* SNPs (Table 1). PBMC from the patient groups were then assessed for autophagy activity by flow cytometry. No significant differences in basal autophagy activity were observed, and azathioprine treatment resulted in an accumulation of autophagosome-bound LC3-II in PBMC from all patient groups (Figure 7A, panel i). Analysis of basal autophagy activity in untreated monocytes revealed no difference across the patient groups and azathioprine treatment again enhanced the accumulation of autophagosome-bound LC3-II (Figure 7A, panel ii). Similar results were observed in monocyte subsets, in addition to T cells, B cells and NK cells (Figure S4). Interestingly, activation of autophagy by azathioprine was not attenuated in PBMC heterozygous or homozygous for the *ATG16L1 T300A* SNP (Figure 7A, panel iii). The low frequency of NOD2 SNPs present in the cohort precluded analysis of effect on azathioprine-induced autophagy. Taken together, these results demonstrate that azathioprine activates autophagy in primary cells *ex vivo*, supporting our *in vitro* findings.

Discussion

The strong association of CD with autophagy genes has led to a substantial amount research demonstrating several key functions for autophagy including regulation of the innate and adaptive immune responses, regulation of the intestinal microbiome and resolution of ER-stress [9,10]. Impaired autophagy responses have been observed in a range of cell types derived from CD patients [10], and there is mounting evidence that inducing autophagy can have therapeutic benefits for the treatment of IBD in both pediatric and adult patients, with several recent studies investigating the utility of mTORC1 inhibitors [12,13,38]. Despite these advances in understanding, there is still little known about how drugs currently approved for clinical use in IBD affect autophagy function.

To evaluate current IBD drugs in the context of autophagy we initially screened for the accumulation of autophagosomes using live cell imaging and identified azathioprine and infliximab as potential modulators of autophagy. However, further investigation using flow cytometry to measure the active, lipidated form of LC3-II revealed that only azathioprine activated the autophagy pathway. Furthermore, results with the GFP-RFP-LC3 plasmid demonstrate that autophagic flux is enhanced in the presence of azathioprine.

Thiopurines are a class of immunosuppressant drugs that includes azathioprine, mercaptopurine (6-MP), and thioguanine (6-TG). It is well-established that thiopurines can inhibit DNA/RNA synthesis and deactivate pro-inflammatory T-lymphocytes [17,18], however, their mechanism of action is not fully understood. Interestingly, several previous studies have also found that thiopurines can activate autophagy primarily via DNA mismatched repair processes in response to DNA damage [9]. To date, only one study has shown autophagy

induction mediated by azathioprine, in colorectal carcinoma cells [39]. The authors suggest that increased autophagy associated with thiopurine exposure is a survival mechanism to compensate for a primary effect on apoptosis and mitochondrial damage. Mechanistically, we show an alternative autophagy-associated process whereby azathioprine increased the expression of several UPR genes including PERK, ATF4 and CHOP as well as expression of the ER-stress chaperone protein PDI. Importantly, we demonstrate that azathioprine induces autophagy independent of apoptosis.

The ER-stress/UPR pathways play an essential role in the maintenance of intestinal homeostasis and genetic studies have identified several ER-stress/UPR genes associated with IBD [33]. Significantly, ER-stress levels are increased in ileal and colonic biopsies from CD patients [40–43]. The UPR acts to maintain ER-homeostasis, and cells that naturally secrete large amounts of protein, such as Paneth cells strongly linked to ileal CD are more susceptible to ER-stress and therefore rely heavily on the UPR [44] .

The UPR and autophagy are intimately linked processes [45], to relieve ER-stress the UPR can induce autophagy to degrade misfolded proteins and protein aggregates [46–50]. Importantly, the major risk factors for CD, NOD2 and ATG16L1, functionally intersect with ER-stress and the UPR [51 52], and ER stress is a significant risk when autophagy or the UPR is not functional. The convergence between autophagy and UPR pathways provides new opportunity for the treatment of IBD and the modulation of the UPR in combination with autophagy is a promising therapeutic strategy. In support of this idea, several recent studies have demonstrated beneficial effects of enhancing UPR function for intestinal homeostasis [53–55].

We also show that azathioprine modulates mTORC1 signaling. A growing body of work suggests that the UPR is regulated by diverse stimuli independently of ER-stress [56] and

stressors such as nutrient deprivation and hypoxia have been shown to activate UPR signaling and inhibit mTORC1 [57]. UPR activation can occur both upstream and downstream of mTORC1 [57], and mTORC1 inhibitors, including rapamycin, are reported to induce PERK and eIF2α activation [58]. Our finding that PERK inhibition did not affect the mTORC1 response to azathioprine suggests that mTORC1 may be acting upstream or in parallel to PERK. Significantly, azathioprine-induced autophagy was reduced in the presence of PERK inhibitor, supporting others findings that PERK regulates LC3B and ATG5 expression [59]. Our results suggest that azathioprine is acting through a pathway that involves both mTORC1 and PERK, and may have synergistic outcomes; mTORC1 inhibition and PERK-eIF2α stimulation may work together to inhibit global protein translation, while mTORC1 inhibition together with increased expression of autophagy genes by PERK [60,61], may result in a general increase in autophagic activity.

AIEC are prevalent in ileal mucosa of CD patients [62] and are able to survive and replicate within macrophages, resulting in sustained inflammatory responses [63] and granuloma formation [64]. Using a CD mucosa-associated strain of AIEC we show that azathioprine enhances the clearance of intracellular bacteria from THP-1 derived macrophages independent of direct effects on bacterial growth. Importantly, AIEC clearance correlated with increased autophagy and reduced pro-inflammatory cytokine gene expression. These combined effects of azathioprine may make it a preferred therapeutic option for subsets of patients with confirmed AIEC infection.

Finally, we carried out an observational study of a clinical cohort of children. PBMC from non-IBD patients or patients with the diagnosis of IBD were analysed to determine basal autophagy levels and response to azathioprine treatment *ex vivo*. Our flow cytometry results

revealed that basal autophagy levels and azathioprine-induced autophagy were similar in all patient groups. Similar results were also observed when we analysed subsets of monocytes, T cells, B cells and NK cells. Importantly, it has been shown that autophagy is required for the differentiation of monocytes to macrophages [65], and for the induction of macrophages which display immunosuppressive and wound healing properties [66]. Our results suggest that enhancing autophagy with azathioprine may promote the induction of macrophages with an anti-inflammatory phenotype irrespective of diagnosis.

Greater understanding of the genetic factors that underlie CD pathogenesis are leading to improvements in treatment, and genotyping for key SNPs in genes involved in both the autophagy and ER-stress/UPR pathways may help to predict patient response to drugs. For example, recent studies have identified an association between *ATG16L1 T300A* SNP and an enhanced therapeutic effect of thiopurines [67] and anti-TNF-α therapy [68]. Interestingly, the immunoregulatory effects of these drugs were associated with autophagy stimulation [66,67,69]. For instance, cytoskeletal defects that reduced mobility in autophagy-deficient DC harbouring the *ATG16L1 T300A* SNP were reversed by thiopurine inhibition of Ras-related C3 botulinum toxin substrate 1 (RAC1) [67]. Significantly, analysis of ATG16L1 genotype in our pediatric cohort revealed that the autophagy response to azathioprine was not attenuated in PBMC from patients carrying the CD-associated *T300A* SNP. The ATG16L1 T300A risk variant confers greater risk for CD in pediatric patients than in adult patients [70,71] , therefore it will be interesting to compare results in PBMC from an adult cohort. Collectively, our studies suggest that patients harbouring the *ATG16L1* risk variant may benefit from thiopurines via mechanisms involving RAC1 inhibition and the induction of autophagy.

Conclusion

Breakdown of the ER-stress/UPR and autophagy pathways has been strongly linked to pathogenesis of IBD. Together, our results suggest that stimulation of autophagy and the UPR may contribute to the therapeutic efficacy of azathioprine. Additional studies are now required to further elucidate how thiopurines modulate these converging pathways; results of these studies may pave the way for development of the next generation of drugs aimed at modulation of the UPR in combination with autophagy.

Autophagy is a cell type specific process, therefore it is essential to assess whether thiopurines modulate autophagy and the UPR in other cell types of direct relevance to IBD, such as Paneth cells strongly linked to ileal CD. Specifically, studies conducted in cells from patients with known CD-associated mutations in the genes regulating the ER-stress/UPR and autophagy pathways will help to identify patients that are most likely to respond.

Acknowledgements

We thank Prof Kenny Simpson (Cornell University, USA) for *E.coli* strains, Prof Ilan Rosenshine, (The Hebrew University of Jerusalem) for the x-light EGFP plasmid and David Hoole (Royal Hospital for Sick Children) for Infliximab. We thank Dr Clare Taylor (Edinburgh Napier University) for advice and continued support. This work was supported by a Crohn's in Childhood Research Association (CICRA) PhD studentship to KMH and by an NHS Research Scotland (NRS) Career Researcher Fellowship to PH.

Authors contributions

KMH, VC and SK conducted the experiments; PH collected clinical specimens.

KMH and CS wrote the manuscript.

KMH, VC, SK, KS, JS, PGB, PH and CS made substantial contributions to conception and design, and/or analysis and interpretation of data.

KMH, VC, SK, KS, JS, PGB, PH and CS reviewed the manuscript critically for important intellectual content.

Competing interests and financial disclosure

The authors declare that we have no competing interests. We have no financial relationships with any organisations that might have an interest in the submitted work.

References

1. NHS CB. *2013/14 NHS Standard Contract for Colorectal: Complex Inflammatory Bowel Disease (Adult)*. 2013.

2. Boyapati R, Satsangi J, Ho GT. Pathogenesis of Crohn's disease. *F1000Prime Rep*. 2015;7:44.

3. Frank DN, Robertson CE, Hamm CM, et al. Disease phenotype and genotype are associated with shifts in intestinal-associated microbiota in inflammatory bowel diseases. *Inflamm. Bowel Dis.* 2011;17:179–184.

4. Darfeuille-Michaud A, Boudeau J, Bulois P, et al. High prevalence of adherent-invasive Escherichia coli associated with ileal mucosa in Crohn's disease. *Gastroenterology*. 2004;127:412–421.

5. Lange KM de, Moutsianas L, Lee JC, et al. Genome-wide association study implicates immune activation of multiple integrin genes in inflammatory bowel disease. *Nat. Genet.* 2017;49:256–261.

6. Franke A, McGovern DP, Barrett JC, et al. Genome-wide meta-analysis increases to 71 the number of confirmed Crohn's disease susceptibility loci. *Nat Genet*. 2010;42:1118–25.

7. Lamb CA, Yoshimori T, Tooze SA. The autophagosome: origins unknown, biogenesis complex. *Nat. Rev. Mol. Cell Biol.* 2013;14:759–774.

8. Deretic V, Saitoh T, Akira S. Autophagy in infection, inflammation and immunity. *Nat Rev Immunol*. 2013;13:722–37.

9. Hooper KM, Barlow PG, Stevens C, et al. Inflammatory Bowel Disease Drugs: A Focus on Autophagy. *J. Crohns Colitis*. 2017;11:118–127.

10. Ke P, Shao B-Z, Xu Z-Q, et al. Intestinal Autophagy and Its Pharmacological Control in Inflammatory Bowel Disease. *Front. Immunol.* 2017;7.

11. Massey DC, Bredin F, Parkes M. Use of sirolimus (rapamycin) to treat refractory Crohn's disease. *Gut*. 2008;57:1294–6.

12. Dumortier J, Lapalus M-G, Guillaud O, et al. Everolimus for refractory Crohn's disease: A case report: *Inflamm. Bowel Dis.* 2008;14:874–877.

13. Mutalib M, Borrelli O, Blackstock S, et al. The use of sirolimus (rapamycin) in the management of refractory inflammatory bowel disease in children. *J. Crohns Colitis*. 2014;8:1730–1734.

14. Bernstein CN, Loftus EV Jr, Ng SC, et al. Hospitalisations and surgery in Crohn's disease. *Gut*. 2012;61:622–9.

15. Bassi A, Dodd S, Williamson P, et al. Cost of illness of inflammatory bowel disease in the UK: a single centre retrospective study. *Gut*. 2004;53:1471–8.

16. Denson LA, Long MD, McGovern DP, et al. Challenges in IBD research: update on progress and prioritization of the CCFA's research agenda. *Inflamm Bowel Dis*. 2013;19:677–82.

17. Tiede I, Fritz G, Strand S, et al. CD28-dependent Rac1 activation is the molecular target of azathioprine in primary human CD4+ T lymphocytes. *J. Clin. Invest.* 2003;111:1133–1145.

18. Swann PF, Waters TR, Moulton DC, et al. Role of Postreplicative DNA Mismatch Repair in the Cytotoxic Action of Thioguanine. *Science*. 1996;273:1109–1111.

19. Kabeya Y, Mizushima N, Ueno T, et al. LC3, a mammalian homologue of yeast Apg8p, is localized in autophagosome membranes after processing. *EMBO J.* 2000;19:5720–5728.

20. Kimura S, Noda T, Yoshimori T. Dissection of the autophagosome maturation process by a novel reporter protein, tandem fluorescent-tagged LC3. *Autophagy*. 2007;3:452–460.

21. Mills E, Baruch K, Aviv G, et al. Dynamics of the type III secretion system activity of enteropathogenic Escherichia coli. *MBio*. 2013;4:e00303–13.

22. Schindelin J, Arganda-Carreras I, Frise E, et al. Fiji: an open-source platform for biological-image analysis. *Nat. Methods*. 2012;9:676–682.

23. Eng KE, Panas MD, Karlsson Hedestam GB, et al. A novel quantitative flow cytometry-based assay for autophagy. *Autophagy*. 2010;6:634–641.

24. Jacob MC, Favre M, Bensa JC. Membrane cell permeabilization with saponin and multiparametric analysis by flow cytometry. *Cytometry*. 1991;12:550–558.

25. Vandesompele J, De Preter K, Pattyn F, et al. Accurate normalization of real-time quantitative RT-PCR data by geometric averaging of multiple internal control genes. *Genome Biol.* 2002;3:research0034.

26. Livak KJ, Schmittgen TD. Analysis of relative gene expression data using real-time quantitative PCR and the 2(-Delta Delta C(T)) Method. *Methods San Diego Calif*. 2001;25:402–408.

27. Simpson KW, Dogan B, Rishniw M, et al. Adherent and invasive Escherichia coli is associated with granulomatous colitis in boxer dogs. *Infect. Immun.* 2006;74:4778–4792.

28. Levine A, Koletzko S, Turner D, et al. ESPGHAN revised porto criteria for the diagnosis of inflammatory bowel disease in children and adolescents. *J. Pediatr. Gastroenterol. Nutr.* 2014;58:795–806.

29. Musiwaro P, Smith M, Manifava M, et al. Characteristics and requirements of basal autophagy in HEK 293 cells. *Autophagy*. 2013;9:1407–1417.

30. Klionsky DJ, Abdelmohsen K, Abe A, et al. Guidelines for the use and interpretation of assays for monitoring autophagy (3rd edition). *Autophagy*. 2016;12:1–222.

31. Mizushima N, Yoshimori T, Levine B. Methods in Mammalian Autophagy Research. *Cell*. 2010;140:313–326.

32. Mariño G, Niso-Santano M, Baehrecke EH, et al. Self-consumption: the interplay of autophagy and apoptosis. *Nat. Rev. Mol. Cell Biol.* 2014;15:81–94.

33. McGuckin MA, Eri RD, Das I, et al. ER stress and the unfolded protein response in intestinal inflammation. *Am. J. Physiol. - Gastrointest. Liver Physiol.* 2010;298:G820–G832.

34. Laplante M, Sabatini DM. mTOR Signaling in Growth Control and Disease. *Cell*. 2012;149:274–293.

35. Avivar-Valderas A, Bobrovnikova-Marjon E, Diehl JA, et al. Regulation of autophagy during ECM detachment is linked to a selective inhibition of mTORC1 by PERK. *Oncogene*. 2013;32:4932–4940.

36. Ji G, Yu N, Xue X, et al. PERK-mediated Autophagy in Osteosarcoma Cells Resists ER Stress-induced Cell Apoptosis. *Int. J. Biol. Sci.* 2015;11:803–812.

37. Palmela C, Chevarin C, Xu Z, et al. Adherent-invasive *Escherichia coli* in inflammatory bowel disease. *Gut*. 2017:gutjnl-2017-314903.

38. Anon. Massey, D C OBredin, FParkes, MengG0800383/Medical Research Council/United KingdomEnglandGut. 2008 Sep;57(9):1294-6. doi.

39. Chaabane W, Appell ML, Chaabane W, et al. Interconnections between apoptotic and autophagic pathways during thiopurine-induced toxicity in cancer cells: the role of reactive oxygen species. *Oncotarget*. 2016;7:75616–75634.

40. Deuring JJ, de Haar C, Koelewijn CL, et al. Absence of ABCG2-mediated mucosal detoxification in patients with active inflammatory bowel disease is due to impeded protein folding. *Biochem. J.* 2012;441:87–93.

41. Kaser A, Lee A-H, Franke A, et al. XBP1 Links ER Stress to Intestinal Inflammation and Confers Genetic Risk for Human Inflammatory Bowel Disease. *Cell*. 2008;134:743–756.

42. Rolhion N, Barnich N, Bringer M-A, et al. Abnormally expressed ER stress response chaperone Gp96 in CD favours adherent-invasive Escherichia coli invasion. *Gut*. 2010;59:1355–1362.

43. Shkoda A, Ruiz PA, Daniel H, et al. Interleukin-10 Blocked Endoplasmic Reticulum Stress in Intestinal Epithelial Cells: Impact on Chronic Inflammation. *Gastroenterology*. 2007;132:190–207.

44. Adolph TE, Tomczak MF, Niederreiter L, et al. Paneth cells as a site of origin for intestinal inflammation. *Nature*. 2013;503(7475):272-6.

45. Hooper KM, Barlow PG, Henderson P, et al. Interactions Between Autophagy and the Unfolded Protein Response: Implications for Inflammatory Bowel Disease. *Inflamm. Bowel Dis.* 2018; doi: 10.1093/ibd/izy380.

46. Hart LS, Cunningham JT, Datta T, et al. ER stress–mediated autophagy promotes Myc-dependent transformation and tumor growth. *J. Clin. Invest.* 2012;122:4621–4634.

47. Li J, Ni M, Lee B, et al. The unfolded protein response regulator GRP78/BiP is required for endoplasmic reticulum integrity and stress-induced autophagy in mammalian cells. *Cell Death Differ.* 2008;15:1460–1471.

48. Ogata M, Hino S, Saito A, et al. Autophagy is activated for cell survival after endoplasmic reticulum stress. *Mol Cell Biol*. 2006;26:9220–31.

49. Shimodaira Y, Takahashi S, Kinouchi Y, et al. Modulation of endoplasmic reticulum (ER) stress-induced autophagy by C/EBP homologous protein (CHOP) and inositol-requiring enzyme 1α (IRE1α) in human colon cancer cells. *Biochem. Biophys. Res. Commun.* 2014;445:524–533.

50. Wang W, Kang H, Zhao Y, et al. Targeting autophagy sensitizes BRAF-mutant thyroid cancer to vemurafenib. *J. Clin. Endocrinol. Metab.* 2016:jc.2016-1999.

51. Keestra-Gounder AM, Byndloss MX, Seyffert N, et al. NOD1 and NOD2 signalling links ER stress with inflammation. *Nature*. 2016;532:394–397.

52. Deuring JJ, Fuhler GM, Konstantinov SR, et al. Genomic ATG16L1 risk allele-restricted Paneth cell ER stress in quiescent Crohn's disease. *Gut*. 2014;63:1081–1091.

53. Cao SS, Zimmermann EM, Chuang B, et al. The Unfolded Protein Response and Chemical Chaperones Reduce Protein Misfolding and Colitis in Mice. *Gastroenterology*. 2013;144:989-1000.e6.

54. Boyce M, Bryant KF, Jousse C, et al. A selective inhibitor of eIF2alpha dephosphorylation protects cells from ER stress. *Science*. 2005;307:935–939.

55. Okazaki T, Nishio A, Takeo M, et al. Inhibition of the dephosphorylation of eukaryotic initiation factor 2α ameliorates murine experimental colitis. *Digestion*. 2014;90:167–178.

56. Rutkowski DT, Hegde RS. Regulation of basal cellular physiology by the homeostatic unfolded protein response. *J. Cell Biol.* 2010;189:783–794.

57. Appenzeller-Herzog C, Hall MN. Bidirectional crosstalk between endoplasmic reticulum stress and mTOR signaling. *Trends Cell Biol.* 2012;22:274–282.

58. Freis P, Bollard J, Lebeau J, et al. mTOR inhibitors activate PERK signaling and favor viability of gastrointestinal neuroendocrine cell lines. *Oncotarget*. 2017;8:20974–20987.

59. Rouschop KMA, Beucken T van den, Dubois L, et al. The unfolded protein response protects human tumor cells during hypoxia through regulation of the autophagy genes MAP1LC3B and ATG5. *J. Clin. Invest.* 2010;120:127–141.

60. B'chir W, Maurin A-C, Carraro V, et al. The eIF2α/ATF4 pathway is essential for stress-induced autophagy gene expression. *Nucleic Acids Res.* 2013;41:7683–7699.

61. Kouroku Y, Fujita E, Tanida I, et al. ER stress (PERK/eIF2 [alpha] phosphorylation) mediates the polyglutamine-induced LC3 conversion, an essential step for autophagy formation. *Cell Death Differ.* 2007;14:230.

62. Thomazini CM, Samegima DAG, Rodrigues MAM, et al. High prevalence of aggregative adherent Escherichia coli strains in the mucosa-associated microbiota of patients with inflammatory bowel diseases. *Int. J. Med. Microbiol.* 2011;301:475–479.

63. Lapaquette P, Bringer M-A, Darfeuille-Michaud A. Defects in autophagy favour adherent-invasive Escherichia coli persistence within macrophages leading to increased pro-inflammatory response. *Cell. Microbiol.* 2012;14:791–807.

64. Meconi S, Vercellone A, Levillain F, et al. Adherent-invasive Escherichia coli isolated from Crohn's disease patients induce granulomas in vitro. *Cell. Microbiol.* 2007;9:1252–1261.

65. Zhang Y, Morgan MJ, Chen K, et al. Induction of autophagy is essential for monocyte-macrophage differentiation. *Blood*. 2012;119:2895–2905.

66. Levin AD, Koelink PJ, Bloemendaal FM, et al. Autophagy Contributes to the Induction of Anti-TNF Induced Macrophages. *J. Crohns Colitis*. 2016;10:323–329.

67. Wildenberg ME, Koelink PJ, Diederen K, et al. The ATG16L1 risk allele associated with Crohn's disease results in a Rac1-dependent defect in dendritic cell migration that is corrected by thiopurines. *Mucosal Immunol.* 2017;10:352–360.

68. Wildenberg M, Levin A, Vos C, et al. P668 ATG16L1 genotype is associated with response to anti-TNF in vitro. *J. Crohns Colitis*. 2013;7:S279.

69. Vos ACW, Wildenberg ME, Arijs I, et al. Regulatory macrophages induced by infliximab are involved in healing in vivo and in vitro. *Inflamm. Bowel Dis.* 2012;18:401–408.

70. Amre DK, Mack DR, Morgan K, et al. Autophagy gene ATG16L1 but not IRGM is associated with Crohn's disease in Canadian children. *Inflamm. Bowel Dis.* 2009;15:501–507.

71. Zhang H-F, Qiu L-X, Chen Y, et al. ATG16L1 T300A polymorphism and Crohn's disease susceptibility: evidence from 13,022 cases and 17,532 controls. *Hum. Genet.* 2009;125:627–631.

72. Levine A, Griffiths A, Markowitz J, et al. Pediatric modification of the Montreal classification for inflammatory bowel disease: the Paris classification. *Inflamm. Bowel Dis.* 2011;17:1314–1321.

674

Abbreviations

5-ASA	Aminosalicylates
AIEC	Adherent Invasive *E. coli*
ATF6	Activating transcription factor 6
ATG16L1	Autophagy-related protein 16-1
BafA1	Bafilomycin A1
BiP/Grp78	Binding immunoglobulin protein/78-kDa glucose-regulated protein
CD	Crohn's disease
CFU	Colony forming units
DAPI	4',6'-diamidino-2-phenylindole
DC	Dendritic cell
DMEM	Dulbecco's modified Eagle medium
EBSS	Earle's Balanced Salt Solution
E. coli	*Escherichia coli*
EIF2a	Eukaryotic translation initiation factor 2A
ER	Endoplasmic Reticulum
FBS	Foetal bovine serum
GI	Gastrointestinal tract
GWAS	Genome-wide association studies
IBD	Inflammatory Bowel Disease
IBDU	IBD-unclassified
IPTG	isopropyl β-D-1-thiogalactopyranosid
IRE1α	Inositol-requiring enzyme 1α

IRGM	Immunity-related GTPase family M protein
LC3	MAP1LC3B
mTORC1	Mechanistic target of rapamycin
MOI	Multiplicity of infection
NOD2	Nucleotide-binding oligomerisation domain-containing protein 2
PBMC	Peripheral blood mononuclear cells
PDI	Protein disulphide isomerase
PERK	Protein kinase R (PKR)-like endoplasmic reticulum kinase
PFA	Paraformaldehyde
PMA	Phorbol myristate acetate
RAC1	Ras-related C3 botulinum toxin substrate 1
p-rpS6	Phosphorylated ribosomal protein S6
TNF-α	Tumour necrosis factor alpha
UC	Ulcerative colitis
UPR	Unfolded protein response
XBP1	x-box-binding protein 1

Table 1. Pediatric patient genotype

CD Crohn's disease, *UC* Ulcerative colitis, *IBDU* IBD unclassified. *ATG16L1 T300A* genotype: rs2241880. **NOD2* genotype SNPs: *L1007fs* (rs2241880), *G908R* (rs2066845) and *R702W* (rs2066844).

	Non-IBD	CD	UC	IBDU
Cohort (n=29)	9	12	7	1
Genotype *ATG16L1 T300A* (n=26)				
Wildtype	1	2	1	N/A
Heterozygous risk	3	6	3	N/A
Homozygous risk	3	4	3	N/A
Genotype *NOD2 L1007fs* (n=27)				
Wildtype	8	12	7	N/A
Heterozygous risk	0	0	0	N/A
Homozygous risk	0	0	0	N/A
Genotype *NOD2 G908R* (n=27)				
Wildtype	8	11	7	N/A
Heterozygous risk	0	0	0	N/A
Homozygous risk	0	1	0	N/A
Genotype *NOD2 R702W* (n=27)				
Wildtype	7	11	6	N/A
Heterozygous risk	0	1	0	N/A
Homozygous risk	1	0	1	N/A

719

Figure Legends

Figure 1: Modulation of autophagy by current IBD drugs

HEK293 GFP-LC3 cells were untreated (i) or treated with DMSO (ii), EBSS (iii), 120μM Azathioprine (iv and x), 100μg/ml Infliximab (v and xi), 120μM Methotrexate (vi and xii), 100μM methylprednisolone (vii and xiii) or 150μM sulfasalazine (viii and xiv) and assessed by live-cell confocal microscopy up to 12hr. 50 cells counted from 3 fields of view and percentage cells with >5 GFP-LC3 puncta quantified (+/- SEM) for all time-points (x-xiv) with 6hr time-point highlighted **p <0.01; ****p < 0.0001 (ix).

Figure 2: Azathioprine activates the autophagy pathway

A) HEK293 GFP-LC3 cells were treated for 6hr with 160nM BafA1 only or BafA1 plus EBSS (i), BafA1 plus 120μM azathioprine (ii) or BafA1 plus 100μg/ml Infliximab (iii). Geometric mean of GFP-LC3-II intensity was assessed by flow cytometry. Fold-change in GFP-LC3-II geometric mean from BafA1 only was quantified (+/-SEM) (iv).

B) HEK293 cells were transfected with GFP-RFP-LC3 plasmid and left untreated (i, v, ix) or treated with 160nM BafA1 (ii, vi, x), EBSS (iii, vii, xi), or 120μM azathioprine (iv, viii, xii) for 6hr, and imaged by confocal microscopy. Percentage of transfected cells exhibiting >10 LC3 puncta was quantified (+/-SEM) (n=5) (xiii) *p <0.05. Number of (RFP+GFP+) and (RFP+GFP-) LC3 puncta were quantified (+/-SEM) (n=5) (xiv) **p <0.01, ***p <0.001.

Figure 3: Azathioprine induces autophagosome accumulation independent of apoptosis

A) THP-1-derived macrophages were untreated (i), or treated with DMSO (ii), EBSS (iii), or 120μM azathioprine (iv) for 6hr. Cells were then immunostained for endogenous LC3 and imaged by confocal microscopy. 30 cells were counted from 3 fields of view and percentage cells with >5 GFP-LC3 puncta quantified (+/- SEM) *p <0.05; **p < 0.01 (v).

B) THP-1-derived macrophages were left untreated (i, v) or treated with DMSO (ii, vi), 120μM azathioprine (iii, vii) or 30μM camptothecin (iv, viii) for 6hr (i-iv) and 24hr (v-vii). Cells were stained with Annexin-V/PI and analysed by flow cytometry. Mean percentage population in each quadrant was quantified (+/- SEM) **p value <0.01, ***p value <0.001, ****p value <0.0001 (ix) compared to untreated for corresponding time-point and quadrant.

Figure 4: Azathioprine stimulates the UPR

THP-1-derived macrophages were left untreated, or treated with DMSO, 60μM or 120μM azathioprine, or EBSS for 2, 4, 6, 16 and 24hr. Expression of PERK was determined by RT-qPCR and is displayed in Log_{10} scale (i). 6hr time-point, including treatment with 0.5μg/ml Brefeldin A quantification (+/- SEM) is shown for PERK (ii), ATF4 (iii), CHOP (iv), PDI (vi) and BiP (vii). Using 2^{-ddct}: *p <0.05, **p <0.01, ****p <0.0001.

Figure 5: Azathioprine modulates autophagy via mechanisms involving mTORC1 and PERK.

A) THP-1-derived macrophages were left untreated or treated with DMSO, azathioprine (60-120μM), EBSS or the mTORC1 inhibitor rapamycin (100nM) for 6hr. Protein lysates were immunoblotted for rpS6, phosphorylated rpS6 (p-rpS6 (S235/236)) and actin (i). rpS6/p-rpS6 density normalized to actin was quantified as a percentage of untreated (ii). Representative blot from n=3.

B) THP-1-derived macrophages were left untreated, or treated with DMSO, 120μM azathioprine, EBSS, or 0.5μg/ml Brefeldin A for 6hr in the absence or presence of PERK inhibitor. Protein lysates were immunoblotted for rpS6, phosphorylated rpS6 (p-rpS6 (S235/236)), phosphorylated eIF2α (p-eIF2α (S51) and tubulin (i). rpS6/p-rpS6 density (ii) and p-eIF2α density (iii) normalized to tubulin was quantified. Representative blot from n=3.

C) THP-1-derived macrophages were left untreated, or treated with 120μM azathioprine, or EBSS for 6 hr in the absence (i-iii) and presence (iv-vi) of PERK inhibitor and immunostained for LC3. 100 cells were counted per treatment and percentage cells with >5 GFP-LC3 puncta quantified (+/- SEM) *p <0.05 (vii).

Figure 6: Azathioprine enhances clearance of intracellular AIEC and dampens the inflammatory response.

A) THP-1-derived macrophages were infected with AIEC and gentamicin protection assay performed in the absence or presence of DMSO or 120μM azathioprine. CFU/ml of cell lysates were enumerated, and fold-change mean CFU/ml from untreated was calculated (+/- SEM), **p <0.01.

B and C) THP-1-derived macrophages were infected with AIEC-mCherry and gentamicin protection assay performed in the absence or presence of DMSO or 120μM azathioprine. Fluorescent AIEC were enumerated and percentage cells with intracellular bacteria quantified (+/- SEM), *p <0.05, **p <0.01, ***p <0.001.

D) THP-1-derived macrophages were infected with AIEC (i) or treated with 200ng/ml LPS (ii) and left untreated or treated with DMSO or 120μM azathioprine for 6hr. Expression of TNF-α

was normalized to untreated and mean fold-change expression quantified from n=3 (+/- SEM) (i-ii). Using 2^{-ddct} : *p <0.05.

Figure 7: Azathioprine activates autophagy in PBMC and monocytes from pediatric patients.

PBMC isolated from non-IBD control and IBD patients were left untreated or treated with 120µM azathioprine for 6hr. PBMC were stained with surface markers for classification into populations and for endogenous LC3-II. Geometric mean of LC3-II intensity was quantified by flow cytometry and mean of LC3-II geometric mean (+/-SEM) is shown for total PBMC (I, iii) and total monocytes (ii) for each non-IBD and IBD patient group (i-ii) and each *ATG16L1* genotype (iii**)**. One-way ANOVA with Tukey's multiple comparison was used to compare LC3-II geometric mean between patient groups in untreated cells. Within each patient group paired, two tailed t test was used to compare LC3-II geometric mean of untreated and azathioprine-treated cells. *p < 0.05, **p <0.01.

Table S1: Concentration and manufacturer details of reagents used for cell treatments.

Working concentrations were diluted in appropriate growth media.

Table S2: Antibody details

WB western blot, *IF* immunofluorescent staining, *F* flow cytometry, *IHC* immunohistochemistry. All primary and secondary antibodies were prepared in 1% FBS or goat serum.

Table S3: qPCR Primer Details

FW forward and *RV* reverse primer sequences.

Table S4: Pediatric patient demographics

CD Crohn's disease, *UC* Ulcerative colitis, *IBDU* IBD unclassified. *SD* Standard deviation. *Non-IBD diagnosis included normal (4 patients), mild constipation (1 patient), Irritable Bowel Syndrome (IBS) (3 patients) and threadworms (1 patient). [a]Paris Classification for CD: *L1* ileal, *L2* colonic, *L3* ileocolonic, *L4a* upper disease proximal to ligament of Treitz; *B1* non-stricturing and non-penetrating, *B2* stricturing, *B3* penetrating, *p* perianal disease modifier [72]. [b]Paris Classification for UC: *E1* ulcerative proctitis, *E2* left-sided UC (distal to splenic flexure), *E3* extensive (hepatic flexure distally), *E4* pancolitis (proximal to hepatic flexure); *S0* never severe, *S1* ever severe as defined by Pediatric Ulcerative Colitis Activity Index (PUCAI) [72]. *5-ASA* 5-aminosalisylates.

Figure S1: GFP-LC3 Flow Cytometry in HEK293 GFP-LC3 cells.

Schematic diagram showing cell permeabilization with 0.05% saponin to remove cytosolic GFP-LC3 to allow flow cytometery analysis [23] (i). HEK293 GFP-LC3 cells were either untreated or treated with 160nM bafilomycin for 6 hours. Cells were washed without (ii) or with (iii) cell permeabilization with 0.05% saponin to remove cytosolic GFP-LC3 before fixation. Geometric mean of GFP-LC3 fluorescent intensity of cells was quantified by flow cytometry and analysed using FlowJo software (ii-iii).

Figure S2: Differentially Expressed Genes from RT^2 Profiler™ PCR Array for Human Autophagy Genes when treated with Azathioprine

THP-1-derived macrophages were untreated or treated with 120μM azathioprine for 6 hours. mRNA was extracted and converted to cDNA for RT-qPCR analysis using the RT^2 Profiler™ PCR Array for Human Autophagy genes according to manufacturer instructions. The calibrating sample was untreated cells and relative expression for azathioprine treatment is displayed as fold-change, with upregulated genes calculated as 2^{-ddCT} and downregulated genes as 2^{ddCT}. Differentially expressed genes are shown, with 1.5-fold change in expression considered as the threshold for differential expression.

Figure S3: Effect of azathioprine on growth of AIEC, clearance of intracellular AIEC and pro-inflammatory cytokine responses

LB broth was inoculated from an overnight culture of AIEC to an optical density of 0.05 at 600nm. The cultures were untreated, or treated with DMSO, or 120µM of azathioprine and incubated at 37^{o}C with shaking at 200RPM. Optical density at 600nm was measured every 0.5 hours and plotted in logarithmic scale to show growth phases.

Figure S4: Azathioprine activates autophagy in monocyte subsets, T cells, B cells and NK cells from pediatric patients.

PBMC isolated from non-IBD control and IBD patients were left untreated or treated with 120µM azathioprine for 6h. PBMC were stained with surface markers for classification into populations and for endogenous LC3-II. Geometric mean of LC3-II intensity was quantified by flow cytometry and mean of LC3-II geometric mean (+/-SEM) is shown for classical monocytes (i), intermediate monocytes (ii), non-classical monocytes (iii), T cells (iv), B cells (v) and NK cells (vi) for each non-IBD and IBD patient group. One-way ANOVA with Tukey's multiple comparison was used to compare LC3-II geometric mean between patient groups in untreated cells. Within each patient group paired, two tailed t test was used to compare LC3-II geometric mean of untreated and azathioprine-treated cells. *$p < 0.05$, **$p < 0.01$.

The inflammatory bowel disease drug azathioprine induces autophagy via mTORC1 and the unfolded protein response sensor PERK

Kirsty M. Hooper, PhD[1], Victor Casanova, PhD[1], Sadie Kemp, BSc[1], Katherine A. Staines, PhD[1], Jack Satsangi, FRSE[2,5], Peter G. Barlow, PhD[1], Paul Henderson, MBChB, PhD[3, 4¶] and Craig Stevens, PhD[1¶*].

1. School of Applied Sciences, Edinburgh Napier University, Sighthill Campus, Sighthill Court, Edinburgh, EH11 4BN.

2. Centre for Genomic & Experimental Medicine, University of Edinburgh, Western General Hospital Campus, Crewe Road, Edinburgh EH4 2XU.

3. Child Life and Health, University of Edinburgh, Edinburgh, EH9 1UW.

4. Department of Pediatric Gastroenterology and Nutrition, Royal Hospital for Sick Children, Edinburgh, EH9 1LF.

5. Translational Gastroenterology Unit, Nuffield Department of Medicine, John Radcliffe Hospital, Oxford OX3 9DU.

¶Joint senior authors

17 Short title: The CD drug azathioprine induces autophagy

18

19 Address for correspondence

20 *Dr Craig Stevens

21 School of Applied Sciences, Edinburgh Napier University, Sighthill Campus, Sighthill Court,

22 Edinburgh, EH11 4BN.

23 Email: C.Stevens@napier.ac.uk

24 Tel: 0044 131 455 2930

25

26 Summary

27

28 The aim of this study was to evaluate the effect of current inflammatory bowel disease drugs

29 on autophagy and investigate molecular mechanisms of action and functional outcomes in

30 relation to this cellular process.

31

Abstract

Background: Genetic studies have strongly linked autophagy to Crohn's disease (CD) and stimulating autophagy in CD patients may be therapeutically beneficial. The aim of this study was to evaluate the effect of current inflammatory bowel disease (IBD) drugs on autophagy and investigate molecular mechanisms of action and functional outcomes in relation to this cellular process.

Methods: Autophagy marker LC3 was evaluated by confocal fluorescence microscopy and flow cytometry. Drug mechanism of action was investigated by PCR Array with changes in signaling pathways examined by immunoblot and RT-qPCR. Clearance of adherent-invasive *Escherichia coli* (AIEC) and levels of pro-inflammatory cytokine tumour necrosis factor alpha (TNFα) were evaluated by gentamicin protection assays and RT-qPCR respectively. LC3 was analysed in peripheral blood mononuclear cells (PBMC) from pediatric patients by flow cytometry.

Results: Azathioprine induces autophagy via mechanisms involving modulation of mechanistic target of rapamycin (mTORC1) signaling and stimulation of the unfolded protein response (UPR) sensor PERK. Induction of autophagy with azathioprine correlated with the enhanced clearance of AIEC and dampened AIEC-induced increases in TNFα. Azathioprine induced significant increase in autophagosome bound LC3-II in PBMC populations *ex vivo,* supporting *in vitro* findings. In patients, the CD-associated *ATG16L1 T300A* single-nucleotide polymorphism did not attenuate azathioprine induction of autophagy.

Conclusions: Modulation of autophagy via mTORC1 and the UPR may contribute to the therapeutic efficacy of azathioprine in IBD.

Keywords: Azathioprine, autophagy, mTORC1, unfolded protein response, Adherent-invasive *E.coli*.

Introduction

The inflammatory bowel diseases (IBD), Crohn's disease (CD), ulcerative colitis (UC) and IBD-unclassified (IBDU), are characterized by chronic inflammation of the gastrointestinal (GI) tract and have a prevalence of up to 400 per 100,000 people in the United Kingdom [1]. The pathogenesis of IBD is multifactorial in nature, with genetic predisposition, breakdown of the intestinal epithelial barrier, and concomitant interaction with environmental triggers in the lumen contributing to disease[2]. A dysregulated immune response to intestinal microflora has been heavily implicated, and examination of the disease-associated microbiome has identified several potentially causative agents [3]. Most notably *Escherichia coli* (*E.coli)* strains with an adherent and invasive phenotype (AIEC) have been consistently isolated by independent investigators from CD patients with ileal disease [4].

Genome-wide association studies (GWAS) have identified 240 IBD susceptibility loci to date[5] and have confirmed association with previously recognized susceptibility genes including *Nucleotide-binding oligomerisation domain-containing protein 2 (NOD2)*. Amongst genes identified are several linked to autophagy including *autophagy-related protein* (*ATG*)*16L1, Immunity-related GTPase family M protein* (*IRGM*) and *leucine rich repeat kinase 2* (*LRRK2*) [6]. Autophagy is an intracellular homeostatic process that involves the formation and maturation of double membrane vesicles, known as autophagosomes, which engulf cargo that is degraded upon fusion with lysosomes [7]. Autophagy can be an important survival mechanism that is induced in response to a myriad of stresses. Autophagy plays an essential role in the innate and adaptive immune responses and the timely resolution of inflammation [8], and loss of immune regulation is a key event leading to the chronic inflammation observed in CD [9]. Notably, impaired autophagy responses have been observed in a range of cell types derived

from CD patients including the specialized intestinal epithelial cells (IECs) Paneth cells and goblet cells, and leukocytes, such as macrophages and dendritic cells (DC) [10].

Evidence suggests that inducing autophagy may have therapeutic benefit for the treatment of IBD [9]. Mechanistic target of rapamycin complex 1 (mTORC1) is a master regulator of cell growth and a potent inhibitor of autophagy [10], therefore inhibition of mTORC1 with rapamycin or its analogues, sirolimus and everolimus, strongly induces autophagy. In previously reported case studies sirolimus improved symptoms and intestinal healing in a patient with severe refractory CD [11] and everolimus controlled symptoms for 18 months in a patient with refractory UC [12]. In a study of refractory pediatric IBD, sirolimus induced clinical remission in 45% of UC patients and 100% of CD patients [13].

Drugs currently approved for clinical use for IBD, including corticosteroids, immunomodulators, aminosalicylates (5-ASAs) and biologics, target the immune system to reduce inflammation and induce remission, however response to treatment often diminishes over time, with 10–35% of CD patients requiring surgery within a year of diagnosis and up to 61% by 10 years [14]. A National Health Service review estimated IBD treatment costs of £720 million ($940m) per year in the United Kingdom alone [1], with roughly a quarter of these costs directly attributed to drug treatments [15]. The Crohn's and Colitis Foundation has recently highlighted the need for research into optimizing existing medical therapies [16], with patient stratification of key importance in this context [13]. In order to optimize therapies, a more comprehensive understanding of drug mechanisms of action is required.

We aimed to evaluate current IBD drugs in the context of autophagy and show that the immunomodulator azathioprine induces autophagy via mechanisms involving modulation of

103 mTORC1 and stimulation of the unfolded protein response (UPR) sensor PERK. Our results
104 suggest that in addition to well-characterized effects on DNA/RNA synthesis and T-
105 lymphocytes [17,18], modulation of autophagy and the UPR may contribute to the therapeutic
106 efficacy of azathioprine.

107

Materials and Methods

Cell culture, transfection, plasmids and reagents

HEK293 cells were grown in Dulbecco's modified Eagle medium (DMEM) (Gibco, ThermoFisher Scientific, Paisley, UK) supplemented with 10% foetal bovine serum (FBS) (Invitrogen, ThermoFisher Scientific) and penicillin streptomycin (Gibco). The monocytic THP-1 cell line was grown in RPMI 1640 (Sigma-Aldrich, Irvine, UK), supplemented with 10% FBS, penicillin streptomycin and 200mM L-glutamine (Gibco). For differentiation to macrophages, THP-1 cells were incubated in RPMI growth media supplemented with 10ng/ml phorbol myristate acetate (PMA) (Sigma-Aldrich, Dorset, UK) for 48 hr, then rested for 24 hr in fresh RPMI growth media prior to experiments.

For transfection of HEK293 cells, a Nucleofector Kit V (Lonza Ltd, Manchester, UK) was used according to the manufacturer's instructions. The GFP-LC3 [19], GFP-RFP-LC3 [20] and x-light EGFP [21] plasmids have been described previously. All reagents used are detailed in supplementary (Table S1). For nutrient deprivation, cells were incubated with Earle's Balanced Salt Solution (EBSS) (Gibco).

Immunoblotting

Cells were lysed in ice-cold extraction buffer (50mM Tris [pH 7.6], 150mM NaCl, 5mM EDTA, 0.5% NP-40, 5mM NaF, 1mM sodium vanadate, 1 × Pierce Protease Inhibitor Cocktail [Thermo Scientific]) for 30 min followed by centrifugation. Protein lysates were resolved by denaturing electrophoresis on acrylamide/bisacrylamide gels and electro-transferred to Immobilon-FL PVDF membrane (Merck Millpore EMD, Watford, UK). Membranes were incubated with

primary antibodies overnight at 4°C, and after washing, were incubated with a secondary antibody for 1hr at room temperature (RT). Antibody details are provided in (Table S2). Proteins were visualized by incubation with an ECL western blotting analysis system (GE Healthcare) and imaged using a G: BOX system (Syngene, Cambridge, UK). Relative intensity of bands were measured using Image J software [22] (National Institutes of Health, Bethesda, MD, USA).

Confocal fluorescence microscopy

Cells were seeded on 21-mm borosilicate glass cover slips, 8 chamber polystyrene vessel CultureSlides (Falcon, Fisher Scientific, Loughborough, UK) or 35mm imaging dishes (Ibidi, Thistle Scientific, Uddingston, UK). Images were captured using Carl Zeiss LSM880 confocal microscope (Jena, Germany) and images were analysed using Image J software [18] (National Institutes of Health).

For fixed cell imaging: Cells were fixed with 4% paraformaldehyde (PFA) for 15 min, permeabilized with PBS/0.2% Triton X-100 (Sigma Aldrich) and blocked with PBS containing 10% goat's serum (Gibco) and 2.5% Human TruStain FcX (BioLegend, San Diego, USA). Primary antibodies (Table S2) were incubated overnight at 4°C and conjugated secondary antibodies for 1hr at RT. Where appropriate, cells were counterstained with 4',6'-diamidino-2-phenylindole (DAPI) or mounted with Vectashield mounting medium for fluorescence with DAPI (Vector Laboratories, Peterborough, UK).

For live cell imaging: Cells were grown in 35mm imaging dishes (Ibidi) and maintained at 37^{o}C and 5% CO_2 in live-cell imaging chamber attached to Carl Zeiss LSM880 confocal microscope. Images were captured every 2 minutes at x40 magnification over a 12hr time period.

For autophagy assays in HEK293 GFP-LC3 stable cells: The basal threshold number of GFP-LC3 puncta per cell was established as 5, and cells exhibiting ≥5 puncta were regarded as having enhanced autophagy activity.

For tandem fluorescent-tagged GFP-RFP-LC3 assays: Cells were transiently transfected with the GFP-RFP-LC3 plasmid and following designated treatments, the fluorescent autophagy markers GFP-RFP-LC3 or RFP-LC3 were observed using a confocal microscope and the number of (RFP+GFP+) and (RFP+GFP-) puncta per cell determined.

Flow cytometry

Peripheral blood mononuclear cells (PBMC) were seeded in 96-well U-bottom plates and cell lines were seeded in 12-well plates. After treatments, cells were gently detached using 0.05% trypsin or Cell Dissociation Solution Non-enzymatic (Sigma Aldrich) at 37°C for 10 min. Cells were acquired using the BD Biosciences (Oxford, UK) Celesta flow cytometer or the FACSCalibur (BD) and data analysis performed using BD FACsDiva Software or FlowJo software.

Autophagy assay: For HEK293 GFP-LC3, cells were collected then washed in 0.05% w/v saponin (Sigma), diluted in PBS to remove the unbound cytosolic LC3 [23], which does not alter expression of membrane antigens [24], prior to acquisition. For PBMC, cells were collected and blocked with 2.5% Human TruStain FcX in PBS for 20 min, then incubated with PBMC surface markers or IgG isotypes diluted in Brilliant Stain Buffer (BD Horizon) for 25 min, both at RT. Cells were then washed in 0.05% w/v saponin, diluted in PBS to remove the unbound cytosolic LC3, and fixed with 1% PFA for 20 min at 4^{o}C. Cells were washed again with 10% goat serum in 0.05% saponin before overnight incubation with primary LC3 antibody or Rb IgG Isotype

control (Invitrogen) in 1% goat serum in 0.05% saponin at 4°C. Secondary antibody in 1% goat serum in 0.05% saponin was incubated for 30 min at 4°C prior to washing and acquisition.

Annexin-V/PI assay. Cells were stained using the FITC Annexin V Apoptosis Detection Kit I (BD Pharmingen) according to manufacturer's instructions.

RT-qPCR

Cells were scraped into RNAzol RT (Sigma-Aldrich) and total RNA extracted according to manufacturer's instructions. Total RNA was quantified using a NanoDrop 2000 Spectrophotometer (Thermo Scientific) and integrity was assessed using an Agilent 2100 Bioanalyzer (Agilent Technologies, Stockport, UK) with RNA Nano Chips and Agilent RNA 6000 Nano Reagents (Agilent Technologies). mRNA was converted to cDNA using nanoScript 2, Reverse Transcription Premix (PrimerDesign Ltd, Chandler´s Ford, UK) according to manufacturer's instructions. For qPCR analysis of gene expression PrecisionPLUS Mastermix with SYBR green and ROX with inert blue dye (PrimerDesign) was used according to manufacturer's instructions with RT-PCR Grade Water (Invitrogen) and the StepOnePlus Real-time PCR System (Applied Biosystems, ThermoFisher). Primers are detailed in supplementary (Table S3). A geNorm kit (PrimerDesign) was used for the selection of appropriate reference genes (*RPL13A* [*Ribosomal Protein L13a*] and *Actin*) with the qbase+ software [25]. 2^{-ddCT} was used for relative quantification of gene expression [26]. The RT² Profiler PCR Array of Human Autophagy genes (Qiagen, Crawley, UK) was performed according to manufacturer instructions.

Bacterial infection assays

For growth curves: LB was inoculated with *E. coli* strain CUICD541-10 [27] isolated from the ileum of a patient with CD (a kind gift from Prof Kenny Simpson, Cornell University, USA), from an overnight culture to an optical density of 0.05 at 600nM. Cultures were treated appropriately, incubated at 37^{o}C with 200rpm shaking, and optical density was measured at 600nM every 30 min.

For intracellular survival: Cells were infected with CUICD541-10 *E. coli* at a multiplicity of infection (MOI) of 10 for 3hr, incubated for 1hr in 100µg/ml gentamicin (Gibco) to kill extracellular bacteria, then maintained for a further 24hr in 20µg/ml gentamicin, with addition of appropriate treatments for the final 6hr. For colony forming unit (CFU) enumeration, cells were lysed for 10 min using 1% Triton X100 in PBS. Lysates were serially diluted and plated on LB agar plates for overnight incubation at 37°C.

For immunofluorescence: CUICD541-10 *E. coli* transformed with an x-light mCherry plasmid were used and 30 min prior to immunostaining cells were incubated with 0.1mM isopropyl β-D-1-thiogalactopyranosid (IPTG) (Sigma) to promote bacterial fluorescence. IPTG and 5µM Cell Tracker Green BODIPY (Invitrogen) were added for the duration of the live-cell imaging of infected cells.

Patients

Patient recruitment and sample collection was performed at the Royal Hospital for Sick Children in Edinburgh, and processing and analysis was performed at Edinburgh Napier University.

Inclusion criteria were: (1) aged 6-18 years on date of colonoscopy; (2) already confirmed CD, UC or IBDU [28] or undergoing first upper and lower GI endoscopy due to gastrointestinal symptoms suggestive of possible bowel inflammation (e.g. abdominal pain, peri-rectal (PR) bleeding, weight loss). Non-IBD patients were defined as those with both microscopically and macroscopically normal colonoscopy. Patients were excluded if they had previously undergone colonoscopy for anything other than known IBD, were diagnosed with anything other than IBD following a full investigative cycle, or who could not provide written consent. Whole blood samples (maximum 15ml), and saliva samples were collected from patients: 20 IBD cases and 9 non-IBD controls (Table S4). PBMC were isolated from whole blood using Ficoll-Paque PLUS (GE Healthcare Bio-Sciences AB, Uppsala, Sweden) and cultured in RPMI growth media. Saliva samples were collected using Oragene DNA kits (DNA Genotek, Ontario, Canada).

Genotyping

Saliva samples were sent to the Wellcome Trust Clinical Research Facility in Edinburgh for analysis. Once recruitment was completed, DNA was extracted using Isohelix kit and Taqman genotyping for each sample was performed for the following SNPs: *ATG16L1 T300A* (rs2241880), *NOD2 L1007f/s* (p.Leu1007fsX1008) (rs2066847), *NOD2 R702W* (rs2066844) and *NOD2 G908R* (rs2066845).

Statistical analysis

Results are reported as the mean ± SEM assuming normally distributed variables with statistical analysis conducted by using one-way or two-way ANOVA, or paired t-test as appropriate, with GraphPad Prism version 7.0 (GraphPad Software, CA, USA).

Ethics

All samples were collected with local institutional and NHS ethical approvals (reference 16/WW/0210). Eligible patients were approached at least 48hr prior to colonoscopy and following consent were recruited to the study.

Data availability

The datasets generated during and/or analysed during the current study are available from the corresponding author on reasonable request.

Results

Azathioprine induces autophagosome accumulation

To evaluate the modulation of autophagy by IBD drugs we used HEK293 cells, a well-characterized cell line used in autophagy research [29] that were engineered to stably express the autophagy marker LC3 fused to green fluorescent protein (GFP-LC3) [30]. GFP-LC3 puncta accumulation was measured by live-cell imaging (Figure 1A). Significant increases in GFP-LC3 puncta number were observed after treatment with the immunomodulator azathioprine (Figure 1A, panel iv and ix) and the biologic infliximab (Figure 1A, panel v and ix) with an optimal time-point of 6 hr for both drugs (Figure 1A, panel x and xi). Significant increases in GFP-LC3 puncta were also observed with EBSS to induce nutrient deprivation, a strong activator of the autophagy pathway (Figure 1A, panel iii and ix). In contrast, the immunomodulator methotrexate (Figure 1A, panel vi, ix and xii), the corticosteroid methylprednisolone (Figure 1A, panel vii, ix and xiii) and the aminosalicylate sulfasalazine (Figure 1A, panel viii, ix and xiv) had no significant effects on GFP-LC3 puncta accumulation.

Azathioprine activates the autophagy pathway

Autophagosomes can accumulate due to activation or inhibition of the autophagy pathway. To distinguish between these processes, we first employed flow cytometric analysis. To facilitate measurement of autophagy activation by flow cytometry, HEK293 GFP-LC3 cells were washed with the glycoside saponin to permeabilize cell plasma membranes prior to analysis. Plasma membrane permeabilization releases inactive cytosolic LC3, with only the active lipidated form of LC3-II, which is tightly associated with autophagosome membranes,

being retained [23] (Supplementary Figure 1). Additionally, Bafilomycin A1 (BafA1), an inhibitor of autophagosome-lysosome fusion[30], was used to augment LC3-II accumulation. Under these conditions azathioprine clearly enhanced the accumulation of autophagosome-bound GFP-LC3-II (Figure 2A, panel ii and quantified in iv). In contrast, infliximab had only minor additional effect on GFP-LC3-II accumulation (Figure 2A, panel iii and iv).

To further validate that azathioprine-mediated activation of the autophagy pathway, we employed a tandem RFP-GFP-LC3 plasmid [31]. This RFP-GFP-LC3 plasmid utilises the pH difference between the acidic autolysosome (formed by fusion of an autophagosome and lysosome) and the neutral autophagosome, with the pH sensitivity differences exhibited by GFP (labile at acidic pH) and RFP (stable at acidic pH). Thus, this plasmid can be used to monitor progression from the autophagosome (RFP+GFP+) to the autolysosome (RFP+GFP-). HEK293 cells were transfected with RFP-GFP-LC3 plasmid and treated with BafA1, EBSS or azathioprine. As expected, all three treatments caused autophagosomes to accumulate (Figure 2B, panel xvi). Inhibition of autophagosome-lysosome fusion with BafA1 resulted in the accumulation of (RFP+GFP+) puncta, which appear as yellow in the merged image (Figure 2B, panel x, xiii and quantified in xvii), while activation of the pathway with EBSS resulted in an accumulation of (RFP+GFP-) puncta indicating that complete progression through the pathway was taking place (Figure 2B, panel xi, xiv and xvii). Azathioprine treatment resulted in an accumulation of (RFP+GFP-) puncta relative to untreated control (Figure 2B, panel xii, xv and xvii) indicating that azathioprine activates the autophagy pathway.

Azathioprine induces autophagosome accumulation in macrophages independent of apoptosis

As with other biological processes, autophagy is cell-type specific and it is therefore essential to determine how azathioprine modulates the autophagy pathway in cell types of direct relevance to IBD. For this purpose, macrophages derived from THP-1 cells were treated with azathioprine and endogenous LC3 puncta accumulation measured by fixed-cell confocal fluorescence microscopy. In line with our previous results (Figure 1A), azathioprine treatment significantly increased the number of LC3 puncta in THP-1 derived macrophages (Figure 3A, panel iv and v). Autophagy and apoptosis are intimately linked [32], therefore it was also important to determine the effect of azathioprine on apoptosis in these cells. Analysis of Annexin V/PI staining by flow cytometry revealed that azathioprine had no effect on cell viability at either 6 hr or 24 hr treatment (Figure 3B, panel ii, iv, and v). Together, these results demonstrate that azathioprine induces autophagosome accumulation in THP-1 derived macrophages independent of apoptosis.

Azathioprine stimulates the UPR

To gain insight into azathioprine mechanism of action, we used the Human Autophagy RT² Profiler PCR Array. Gene expression was compared in THP-1 derived macrophages either left untreated or treated with azathioprine (Figure S3). Among the genes significantly up-regulated by azathioprine was the UPR-regulating kinase EIF2AK3 (also known as PERK). As endoplasmic reticulum (ER)-stress/UPR genes are strongly associated with IBD this was investigated further [33]. A time-course RT-qPCR experiment identified 6 hr as the optimum time-point for up regulation of PERK, which occurred in a dose-dependent manner (Figure 4, panel i and ii). The expression of genes downstream from PERK (ATF4, and CHOP; Figure 4, panel iii and iv), and the ER stress chaperon protein disulphide isomerase (PDI) (Figure 4, panel

vi) were also up regulated after 6 hr of azathioprine treatment in a dose dependent manner. In contrast, expression of the ER stress chaperone protein binding immunoglobulin protein/78-kDa glucose-regulated protein (BiP/Grp78) was not affected by azathioprine treatment after 6 hr (Figure 4, panel vii) however a minor increase was observed after 24 hr. These results indicate that azathioprine stimulates the UPR.

Azathioprine modulates mTORC1 signaling

mTORC1 is a major regulatory hub balancing cell growth and protein translation with control of autophagy [34]. When active, mTORC1 is a potent inhibitor of autophagy. Therefore, levels of phosphorylated ribosomal protein S6 (p-rpS6), a surrogate marker of mTORC1 activity, were evaluated in THP-1 derived macrophages treated with increasing concentrations of azathioprine. Azathioprine treatment caused a dramatic decrease in p-rpS6 in a dose dependent manner (Figure 5A, lanes 3-6 and quantified in ii). These results suggest that azathioprine treatment inhibits mTORC1 activity.

Azathioprine modulates mTORC1 signaling independent of PERK

PERK has been shown to inhibit mTORC1 in response to ER stress as part of a mechanism to induce autophagy [34–36]. To test whether modulation of mTORC1 observed in response to azathioprine is dependent on PERK, THP-1 derived macrophages were treated in the absence or presence of a pharmacologic inhibitor of PERK. Azathioprine again caused a decrease in p-rpS6, and the PERK inhibitor did not significantly alter this effect (Figure 5B, panel i, compare lanes 3 and 8, and quantified in ii). To confirm PERK inhibitor activity, phosphorylation of eIF2a, a well-characterized substrate of PERK, was assessed (Figure 5B, lanes 6-10 and

quantified in iii). These results suggest that modulation of mTORC1 signaling by azathioprine occurs independent of PERK.

Azathioprine-induced autophagy is modulated by PERK

To determine whether PERK is required for azathioprine-induced autophagy, THP-1 derived macrophages were treated with azathioprine or EBSS in the absence or presence of PERK inhibitor. In the presence of PERK inhibitor, azathioprine-induced autophagy was specifically attenuated (Figure 5C, compare panel ii and v, and quantified in vii) compared to EBSS-induced autophagy (Figure 5C, compare panel iii and vi, and quantified in vii). These results indicate that PERK is an important factor regulating azathioprine-induced autophagy.

Azathioprine enhances clearance of intracellular *AIEC*

Evidence suggests that AIEC play a putative role in CD [37]. Therefore, we evaluated the survival of the CD mucosa-associated AIEC strain CUICD541-10 [27] in THP-1 derived macrophages. Initially, it was determined that azathioprine had no direct effect on bacterial growth (Figure S3). Azathioprine treatment did however cause a significant decrease in bacterial CFU in AIEC infected cells (Figure 6A). Furthermore, immunofluorescence analysis showed a decrease in the percentage of cells infected with bacteria (Figure 6B and C, compare panels iii and iv and quantified in v), which correlated with an increased accumulation of LC3 puncta (Figure 6C panel v) indicating that autophagy was being induced.

Infection of cells with AIEC elicits a strong inflammatory response; therefore, RT-qPCR was used to assess expression of the pro-inflammatory cytokine TNFα in THP-1 derived macrophages infected with AIEC. Expression was significantly up regulated by AIEC infection

and this was reduced when cells were treated with azathioprine (Figure 6D, panel i). Azathioprine also reduced the expression of TNFα in cells treated with bacterial lipopolysaccharide (LPS) (Figure 6D, panel ii) suggesting that azathioprine may affect TNFα expression independent of decreased intracellular bacteria. These results demonstrate that azathioprine enhances the clearance of intracellular AIEC and dampens the elevated cytokine levels observed in response to infection.

Azathioprine activates autophagy in PBMC and monocytes from pediatric patients

Non-IBD, CD and UC patients were genotyped for the CD-associated NOD2 (R702W, G908R, L1007fs) and *ATG16L1 T300A* SNPs (Table 1). PBMC from the patient groups were then assessed for autophagy activity by flow cytometry. No significant differences in basal autophagy activity were observed, and azathioprine treatment resulted in an accumulation of autophagosome-bound LC3-II in PBMC from all patient groups (Figure 7A, panel i). Analysis of basal autophagy activity in untreated monocytes revealed no difference across the patient groups and azathioprine treatment again enhanced the accumulation of autophagosome-bound LC3-II (Figure 7A, panel ii). Similar results were observed in monocyte subsets, in addition to T cells, B cells and NK cells (Figure S4). Interestingly, activation of autophagy by azathioprine was not attenuated in PBMC heterozygous or homozygous for the *ATG16L1 T300A* SNP (Figure 7A, panel iii). The low frequency of NOD2 SNPs present in the cohort precluded analysis of effect on azathioprine-induced autophagy. Taken together, these results demonstrate that azathioprine activates autophagy in primary cells *ex vivo*, supporting our *in vitro* findings.

Discussion

The strong association of CD with autophagy genes has led to a substantial amount research demonstrating several key functions for autophagy including regulation of the innate and adaptive immune responses, regulation of the intestinal microbiome and resolution of ER-stress [9,10]. Impaired autophagy responses have been observed in a range of cell types derived from CD patients [10], and there is mounting evidence that inducing autophagy can have therapeutic benefits for the treatment of IBD in both pediatric and adult patients, with several recent studies investigating the utility of mTORC1 inhibitors [12,13,38]. Despite these advances in understanding, there is still little known about how drugs currently approved for clinical use in IBD affect autophagy function.

To evaluate current IBD drugs in the context of autophagy we initially screened for the accumulation of autophagosomes using live cell imaging and identified azathioprine and infliximab as potential modulators of autophagy. However, further investigation using flow cytometry to measure the active, lipidated form of LC3-II revealed that only azathioprine activated the autophagy pathway. Furthermore, results with the GFP-RFP-LC3 plasmid demonstrate that autophagic flux is enhanced in the presence of azathioprine.

Thiopurines are a class of immunosuppressant drugs that includes azathioprine, mercaptopurine (6-MP), and thioguanine (6-TG). It is well-established that thiopurines can inhibit DNA/RNA synthesis and deactivate pro-inflammatory T-lymphocytes [17,18], however, their mechanism of action is not fully understood. Interestingly, several previous studies have also found that thiopurines can activate autophagy primarily via DNA mismatched repair processes in response to DNA damage [9]. To date, only one study has shown autophagy

induction mediated by azathioprine, in colorectal carcinoma cells [39]. The authors suggest that increased autophagy associated with thiopurine exposure is a survival mechanism to compensate for a primary effect on apoptosis and mitochondrial damage. Mechanistically, we show an alternative autophagy-associated process whereby azathioprine increased the expression of several UPR genes including PERK, ATF4 and CHOP as well as expression of the ER-stress chaperone protein PDI. Importantly, we demonstrate that azathioprine induces autophagy independent of apoptosis.

The ER-stress/UPR pathways play an essential role in the maintenance of intestinal homeostasis and genetic studies have identified several ER-stress/UPR genes associated with IBD [33]. Significantly, ER-stress levels are increased in ileal and colonic biopsies from CD patients [40–43]. The UPR acts to maintain ER-homeostasis, and cells that naturally secrete large amounts of protein, such as Paneth cells strongly linked to ileal CD are more susceptible to ER-stress and therefore rely heavily on the UPR [44] .

The UPR and autophagy are intimately linked processes [45], to relieve ER-stress the UPR can induce autophagy to degrade misfolded proteins and protein aggregates [46–50]. Importantly, the major risk factors for CD, NOD2 and ATG16L1, functionally intersect with ER-stress and the UPR [51 52], and ER stress is a significant risk when autophagy or the UPR is not functional. The convergence between autophagy and UPR pathways provides new opportunity for the treatment of IBD and the modulation of the UPR in combination with autophagy is a promising therapeutic strategy. In support of this idea, several recent studies have demonstrated beneficial effects of enhancing UPR function for intestinal homeostasis [53–55].

We also show that azathioprine modulates mTORC1 signaling. A growing body of work suggests that the UPR is regulated by diverse stimuli independently of ER-stress [56] and

420 stressors such as nutrient deprivation and hypoxia have been shown to activate UPR signaling
421 and inhibit mTORC1 [57]. UPR activation can occur both upstream and downstream of mTORC1
422 [57], and mTORC1 inhibitors, including rapamycin, are reported to induce PERK and eIF2α
423 activation [58]. Our finding that PERK inhibition did not affect the mTORC1 response to
424 azathioprine suggests that mTORC1 may be acting upstream or in parallel to PERK.
425 Significantly, azathioprine-induced autophagy was reduced in the presence of PERK inhibitor,
426 supporting others findings that PERK regulates LC3B and ATG5 expression [59]. Our results
427 suggest that azathioprine is acting through a pathway that involves both mTORC1 and PERK,
428 and may have synergistic outcomes; mTORC1 inhibition and PERK-eIF2α stimulation may
429 work together to inhibit global protein translation, while mTORC1 inhibition together with
430 increased expression of autophagy genes by PERK [60,61], may result in a general increase in
431 autophagic activity.

432 AIEC are prevalent in ileal mucosa of CD patients [62] and are able to survive and replicate within
433 macrophages, resulting in sustained inflammatory responses [63] and granuloma formation [64].
434 Using a CD mucosa-associated strain of AIEC we show that azathioprine enhances the
435 clearance of intracellular bacteria from THP-1 derived macrophages independent of direct
436 effects on bacterial growth. Importantly, AIEC clearance correlated with increased autophagy
437 and reduced pro-inflammatory cytokine gene expression. These combined effects of
438 azathioprine may make it a preferred therapeutic option for subsets of patients with
439 confirmed AIEC infection.

440 Finally, we carried out an observational study of a clinical cohort of children. PBMC from non-
441 IBD patients or patients with the diagnosis of IBD were analysed to determine basal
442 autophagy levels and response to azathioprine treatment *ex vivo*. Our flow cytometry results

443 revealed that basal autophagy levels and azathioprine-induced autophagy were similar in all
444 patient groups. Similar results were also observed when we analysed subsets of monocytes,
445 T cells, B cells and NK cells. Importantly, it has been shown that autophagy is required for the
446 differentiation of monocytes to macrophages [65], and for the induction of macrophages which
447 display immunosuppressive and wound healing properties [66]. Our results suggest that
448 enhancing autophagy with azathioprine may promote the induction of macrophages with an
449 anti-inflammatory phenotype irrespective of diagnosis.

450 Greater understanding of the genetic factors that underlie CD pathogenesis are leading to
451 improvements in treatment, and genotyping for key SNPs in genes involved in both the
452 autophagy and ER-stress/UPR pathways may help to predict patient response to drugs. For
453 example, recent studies have identified an association between *ATG16L1 T300A* SNP and an
454 enhanced therapeutic effect of thiopurines [67] and anti-TNF-α therapy [68]. Interestingly, the
455 immunoregulatory effects of these drugs were associated with autophagy stimulation [66,67,69].
456 For instance, cytoskeletal defects that reduced mobility in autophagy-deficient DC harbouring
457 the *ATG16L1 T300A* SNP were reversed by thiopurine inhibition of Ras-related C3 botulinum
458 toxin substrate 1 (RAC1) [67]. Significantly, analysis of ATG16L1 genotype in our pediatric cohort
459 revealed that the autophagy response to azathioprine was not attenuated in PBMC from
460 patients carrying the CD-associated *T300A* SNP. The ATG16L1 T300A risk variant confers
461 greater risk for CD in pediatric patients than in adult patients [70,71] , therefore it will be
462 interesting to compare results in PBMC from an adult cohort. Collectively, our studies suggest
463 that patients harbouring the *ATG16L1* risk variant may benefit from thiopurines via
464 mechanisms involving RAC1 inhibition and the induction of autophagy.

465 # Conclusion

Breakdown of the ER-stress/UPR and autophagy pathways has been strongly linked to pathogenesis of IBD. Together, our results suggest that stimulation of autophagy and the UPR may contribute to the therapeutic efficacy of azathioprine. Additional studies are now required to further elucidate how thiopurines modulate these converging pathways; results of these studies may pave the way for development of the next generation of drugs aimed at modulation of the UPR in combination with autophagy.

Autophagy is a cell type specific process, therefore it is essential to assess whether thiopurines modulate autophagy and the UPR in other cell types of direct relevance to IBD, such as Paneth cells strongly linked to ileal CD. Specifically, studies conducted in cells from patients with known CD-associated mutations in the genes regulating the ER-stress/UPR and autophagy pathways will help to identify patients that are most likely to respond.

Acknowledgements

We thank Prof Kenny Simpson (Cornell University, USA) for *E.coli* strains, Prof Ilan Rosenshine, (The Hebrew University of Jerusalem) for the x-light EGFP plasmid and David Hoole (Royal Hospital for Sick Children) for Infliximab. We thank Dr Clare Taylor (Edinburgh Napier University) for advice and continued support. This work was supported by a Crohn's in Childhood Research Association (CICRA) PhD studentship to KMH and by an NHS Research Scotland (NRS) Career Researcher Fellowship to PH.

Authors contributions

KMH, VC and SK conducted the experiments; PH collected clinical specimens.

KMH and CS wrote the manuscript.

KMH, VC, SK, KS, JS, PGB, PH and CS made substantial contributions to conception and design, and/or analysis and interpretation of data.

KMH, VC, SK, KS, JS, PGB, PH and CS reviewed the manuscript critically for important intellectual content.

Competing interests and financial disclosure

The authors declare that we have no competing interests. We have no financial relationships with any organisations that might have an interest in the submitted work.

References

1. NHS CB. *2013/14 NHS Standard Contract for Colorectal: Complex Inflammatory Bowel Disease (Adult)*. 2013.

2. Boyapati R, Satsangi J, Ho GT. Pathogenesis of Crohn's disease. *F1000Prime Rep*. 2015;7:44.

3. Frank DN, Robertson CE, Hamm CM, et al. Disease phenotype and genotype are associated with shifts in intestinal-associated microbiota in inflammatory bowel diseases. *Inflamm. Bowel Dis.* 2011;17:179–184.

4. Darfeuille-Michaud A, Boudeau J, Bulois P, et al. High prevalence of adherent-invasive Escherichia coli associated with ileal mucosa in Crohn's disease. *Gastroenterology*. 2004;127:412–421.

5. Lange KM de, Moutsianas L, Lee JC, et al. Genome-wide association study implicates immune activation of multiple integrin genes in inflammatory bowel disease. *Nat. Genet.* 2017;49:256–261.

6. Franke A, McGovern DP, Barrett JC, et al. Genome-wide meta-analysis increases to 71 the number of confirmed Crohn's disease susceptibility loci. *Nat Genet*. 2010;42:1118–25.

7. Lamb CA, Yoshimori T, Tooze SA. The autophagosome: origins unknown, biogenesis complex. *Nat. Rev. Mol. Cell Biol.* 2013;14:759–774.

8. Deretic V, Saitoh T, Akira S. Autophagy in infection, inflammation and immunity. *Nat Rev Immunol*. 2013;13:722–37.

9. Hooper KM, Barlow PG, Stevens C, et al. Inflammatory Bowel Disease Drugs: A Focus on Autophagy. *J. Crohns Colitis*. 2017;11:118–127.

10. Ke P, Shao B-Z, Xu Z-Q, et al. Intestinal Autophagy and Its Pharmacological Control in Inflammatory Bowel Disease. *Front. Immunol.* 2017;7.

11. Massey DC, Bredin F, Parkes M. Use of sirolimus (rapamycin) to treat refractory Crohn's disease. *Gut*. 2008;57:1294–6.

12. Dumortier J, Lapalus M-G, Guillaud O, et al. Everolimus for refractory Crohn's disease: A case report: *Inflamm. Bowel Dis.* 2008;14:874–877.

13. Mutalib M, Borrelli O, Blackstock S, et al. The use of sirolimus (rapamycin) in the management of refractory inflammatory bowel disease in children. *J. Crohns Colitis*. 2014;8:1730–1734.

14. Bernstein CN, Loftus EV Jr, Ng SC, et al. Hospitalisations and surgery in Crohn's disease. *Gut*. 2012;61:622–9.

15. Bassi A, Dodd S, Williamson P, et al. Cost of illness of inflammatory bowel disease in the UK: a single centre retrospective study. *Gut*. 2004;53:1471–8.

16. Denson LA, Long MD, McGovern DP, et al. Challenges in IBD research: update on progress and prioritization of the CCFA's research agenda. *Inflamm Bowel Dis*. 2013;19:677–82.

17. Tiede I, Fritz G, Strand S, et al. CD28-dependent Rac1 activation is the molecular target of azathioprine in primary human CD4+ T lymphocytes. *J. Clin. Invest.* 2003;111:1133–1145.

18. Swann PF, Waters TR, Moulton DC, et al. Role of Postreplicative DNA Mismatch Repair in the Cytotoxic Action of Thioguanine. *Science*. 1996;273:1109–1111.

19. Kabeya Y, Mizushima N, Ueno T, et al. LC3, a mammalian homologue of yeast Apg8p, is localized in autophagosome membranes after processing. *EMBO J.* 2000;19:5720–5728.

20. Kimura S, Noda T, Yoshimori T. Dissection of the autophagosome maturation process by a novel reporter protein, tandem fluorescent-tagged LC3. *Autophagy*. 2007;3:452–460.

21. Mills E, Baruch K, Aviv G, et al. Dynamics of the type III secretion system activity of enteropathogenic Escherichia coli. *MBio*. 2013;4:e00303–13.

22. Schindelin J, Arganda-Carreras I, Frise E, et al. Fiji: an open-source platform for biological-image analysis. *Nat. Methods*. 2012;9:676–682.

23. Eng KE, Panas MD, Karlsson Hedestam GB, et al. A novel quantitative flow cytometry-based assay for autophagy. *Autophagy*. 2010;6:634–641.

24. Jacob MC, Favre M, Bensa JC. Membrane cell permeabilization with saponin and multiparametric analysis by flow cytometry. *Cytometry*. 1991;12:550–558.

25. Vandesompele J, De Preter K, Pattyn F, et al. Accurate normalization of real-time quantitative RT-PCR data by geometric averaging of multiple internal control genes. *Genome Biol.* 2002;3:research0034.

26. Livak KJ, Schmittgen TD. Analysis of relative gene expression data using real-time quantitative PCR and the 2(-Delta Delta C(T)) Method. *Methods San Diego Calif*. 2001;25:402–408.

27. Simpson KW, Dogan B, Rishniw M, et al. Adherent and invasive Escherichia coli is associated with granulomatous colitis in boxer dogs. *Infect. Immun.* 2006;74:4778–4792.

28. Levine A, Koletzko S, Turner D, et al. ESPGHAN revised porto criteria for the diagnosis of inflammatory bowel disease in children and adolescents. *J. Pediatr. Gastroenterol. Nutr.* 2014;58:795–806.

29. Musiwaro P, Smith M, Manifava M, et al. Characteristics and requirements of basal autophagy in HEK 293 cells. *Autophagy*. 2013;9:1407–1417.

30. Klionsky DJ, Abdelmohsen K, Abe A, et al. Guidelines for the use and interpretation of assays for monitoring autophagy (3rd edition). *Autophagy*. 2016;12:1–222.

31. Mizushima N, Yoshimori T, Levine B. Methods in Mammalian Autophagy Research. *Cell*. 2010;140:313–326.

32. Mariño G, Niso-Santano M, Baehrecke EH, et al. Self-consumption: the interplay of autophagy and apoptosis. *Nat. Rev. Mol. Cell Biol.* 2014;15:81–94.

33. McGuckin MA, Eri RD, Das I, et al. ER stress and the unfolded protein response in intestinal inflammation. *Am. J. Physiol. - Gastrointest. Liver Physiol.* 2010;298:G820–G832.

34. Laplante M, Sabatini DM. mTOR Signaling in Growth Control and Disease. *Cell*. 2012;149:274–293.

35. Avivar-Valderas A, Bobrovnikova-Marjon E, Diehl JA, et al. Regulation of autophagy during ECM detachment is linked to a selective inhibition of mTORC1 by PERK. *Oncogene*. 2013;32:4932–4940.

36. Ji G, Yu N, Xue X, et al. PERK-mediated Autophagy in Osteosarcoma Cells Resists ER Stress-induced Cell Apoptosis. *Int. J. Biol. Sci.* 2015;11:803–812.

37. Palmela C, Chevarin C, Xu Z, et al. Adherent-invasive *Escherichia coli* in inflammatory bowel disease. *Gut*. 2017:gutjnl-2017-314903.

38. Anon. Massey, D C OBredin, FParkes, MengG0800383/Medical Research Council/United KingdomEnglandGut. 2008 Sep;57(9):1294-6. doi.

39. Chaabane W, Appell ML, Chaabane W, et al. Interconnections between apoptotic and autophagic pathways during thiopurine-induced toxicity in cancer cells: the role of reactive oxygen species. *Oncotarget*. 2016;7:75616–75634.

40. Deuring JJ, de Haar C, Koelewijn CL, et al. Absence of ABCG2-mediated mucosal detoxification in patients with active inflammatory bowel disease is due to impeded protein folding. *Biochem. J.* 2012;441:87–93.

41. Kaser A, Lee A-H, Franke A, et al. XBP1 Links ER Stress to Intestinal Inflammation and Confers Genetic Risk for Human Inflammatory Bowel Disease. *Cell*. 2008;134:743–756.

42. Rolhion N, Barnich N, Bringer M-A, et al. Abnormally expressed ER stress response chaperone Gp96 in CD favours adherent-invasive Escherichia coli invasion. *Gut*. 2010;59:1355–1362.

43. Shkoda A, Ruiz PA, Daniel H, et al. Interleukin-10 Blocked Endoplasmic Reticulum Stress in Intestinal Epithelial Cells: Impact on Chronic Inflammation. *Gastroenterology*. 2007;132:190–207.

44. Adolph TE, Tomczak MF, Niederreiter L, et al. Paneth cells as a site of origin for intestinal inflammation. *Nature*. 2013;503(7475):272-6.

45. Hooper KM, Barlow PG, Henderson P, et al. Interactions Between Autophagy and the Unfolded Protein Response: Implications for Inflammatory Bowel Disease. *Inflamm. Bowel Dis.* 2018; doi: 10.1093/ibd/izy380.

46. Hart LS, Cunningham JT, Datta T, et al. ER stress–mediated autophagy promotes Myc-dependent transformation and tumor growth. *J. Clin. Invest.* 2012;122:4621–4634.

47. Li J, Ni M, Lee B, et al. The unfolded protein response regulator GRP78/BiP is required for endoplasmic reticulum integrity and stress-induced autophagy in mammalian cells. *Cell Death Differ.* 2008;15:1460–1471.

48. Ogata M, Hino S, Saito A, et al. Autophagy is activated for cell survival after endoplasmic reticulum stress. *Mol Cell Biol*. 2006;26:9220–31.

49. Shimodaira Y, Takahashi S, Kinouchi Y, et al. Modulation of endoplasmic reticulum (ER) stress-induced autophagy by C/EBP homologous protein (CHOP) and inositol-requiring enzyme 1α (IRE1α) in human colon cancer cells. *Biochem. Biophys. Res. Commun.* 2014;445:524–533.

50. Wang W, Kang H, Zhao Y, et al. Targeting autophagy sensitizes BRAF-mutant thyroid cancer to vemurafenib. *J. Clin. Endocrinol. Metab.* 2016:jc.2016-1999.

51. Keestra-Gounder AM, Byndloss MX, Seyffert N, et al. NOD1 and NOD2 signalling links ER stress with inflammation. *Nature*. 2016;532:394–397.

52. Deuring JJ, Fuhler GM, Konstantinov SR, et al. Genomic ATG16L1 risk allele-restricted Paneth cell ER stress in quiescent Crohn's disease. *Gut*. 2014;63:1081–1091.

53. Cao SS, Zimmermann EM, Chuang B, et al. The Unfolded Protein Response and Chemical Chaperones Reduce Protein Misfolding and Colitis in Mice. *Gastroenterology*. 2013;144:989-1000.e6.

54. Boyce M, Bryant KF, Jousse C, et al. A selective inhibitor of eIF2alpha dephosphorylation protects cells from ER stress. *Science*. 2005;307:935–939.

55. Okazaki T, Nishio A, Takeo M, et al. Inhibition of the dephosphorylation of eukaryotic initiation factor 2α ameliorates murine experimental colitis. *Digestion*. 2014;90:167–178.

56. Rutkowski DT, Hegde RS. Regulation of basal cellular physiology by the homeostatic unfolded protein response. *J. Cell Biol.* 2010;189:783–794.

57. Appenzeller-Herzog C, Hall MN. Bidirectional crosstalk between endoplasmic reticulum stress and mTOR signaling. *Trends Cell Biol.* 2012;22:274–282.

58. Freis P, Bollard J, Lebeau J, et al. mTOR inhibitors activate PERK signaling and favor viability of gastrointestinal neuroendocrine cell lines. *Oncotarget*. 2017;8:20974–20987.

638 59. Rouschop KMA, Beucken T van den, Dubois L, et al. The unfolded protein response
639 protects human tumor cells during hypoxia through regulation of the autophagy genes
640 MAP1LC3B and ATG5. *J. Clin. Invest.* 2010;120:127–141.

641 60. B'chir W, Maurin A-C, Carraro V, et al. The eIF2α/ATF4 pathway is essential for stress-
642 induced autophagy gene expression. *Nucleic Acids Res.* 2013;41:7683–7699.

643 61. Kouroku Y, Fujita E, Tanida I, et al. ER stress (PERK/eIF2 [alpha] phosphorylation) mediates
644 the polyglutamine-induced LC3 conversion, an essential step for autophagy formation.
645 *Cell Death Differ.* 2007;14:230.

646 62. Thomazini CM, Samegima DAG, Rodrigues MAM, et al. High prevalence of aggregative
647 adherent Escherichia coli strains in the mucosa-associated microbiota of patients with
648 inflammatory bowel diseases. *Int. J. Med. Microbiol.* 2011;301:475–479.

649 63. Lapaquette P, Bringer M-A, Darfeuille-Michaud A. Defects in autophagy favour adherent-
650 invasive Escherichia coli persistence within macrophages leading to increased pro-
651 inflammatory response. *Cell. Microbiol.* 2012;14:791–807.

652 64. Meconi S, Vercellone A, Levillain F, et al. Adherent-invasive Escherichia coli isolated from
653 Crohn's disease patients induce granulomas in vitro. *Cell. Microbiol.* 2007;9:1252–1261.

654 65. Zhang Y, Morgan MJ, Chen K, et al. Induction of autophagy is essential for monocyte-
655 macrophage differentiation. *Blood*. 2012;119:2895–2905.

656 66. Levin AD, Koelink PJ, Bloemendaal FM, et al. Autophagy Contributes to the Induction of
657 Anti-TNF Induced Macrophages. *J. Crohns Colitis*. 2016;10:323–329.

658 67. Wildenberg ME, Koelink PJ, Diederen K, et al. The ATG16L1 risk allele associated with
659 Crohn's disease results in a Rac1-dependent defect in dendritic cell migration that is
660 corrected by thiopurines. *Mucosal Immunol.* 2017;10:352–360.

661 68. Wildenberg M, Levin A, Vos C, et al. P668 ATG16L1 genotype is associated with response
662 to anti-TNF in vitro. *J. Crohns Colitis*. 2013;7:S279.

663 69. Vos ACW, Wildenberg ME, Arijs I, et al. Regulatory macrophages induced by infliximab are
664 involved in healing in vivo and in vitro. *Inflamm. Bowel Dis.* 2012;18:401–408.

665 70. Amre DK, Mack DR, Morgan K, et al. Autophagy gene ATG16L1 but not IRGM is associated
666 with Crohn's disease in Canadian children. *Inflamm. Bowel Dis.* 2009;15:501–507.

667 71. Zhang H-F, Qiu L-X, Chen Y, et al. ATG16L1 T300A polymorphism and Crohn's disease
668 susceptibility: evidence from 13,022 cases and 17,532 controls. *Hum. Genet.*
669 2009;125:627–631.

670 72. Levine A, Griffiths A, Markowitz J, et al. Pediatric modification of the Montreal
671 classification for inflammatory bowel disease: the Paris classification. *Inflamm. Bowel*
672 *Dis.* 2011;17:1314–1321.

673

674

Abbreviations

5-ASA	Aminosalicylates
AIEC	Adherent Invasive *E. coli*
ATF6	Activating transcription factor 6
ATG16L1	Autophagy-related protein 16-1
BafA1	Bafilomycin A1
BiP/Grp78	Binding immunoglobulin protein/78-kDa glucose-regulated protein
CD	Crohn's disease
CFU	Colony forming units
DAPI	4',6'-diamidino-2-phenylindole
DC	Dendritic cell
DMEM	Dulbecco's modified Eagle medium
EBSS	Earle's Balanced Salt Solution
E. coli	*Escherichia coli*
EIF2a	Eukaryotic translation initiation factor 2A
ER	Endoplasmic Reticulum
FBS	Foetal bovine serum
GI	Gastrointestinal tract
GWAS	Genome-wide association studies
IBD	Inflammatory Bowel Disease
IBDU	IBD-unclassified
IPTG	isopropyl β-D-1-thiogalactopyranosid
IRE1α	Inositol-requiring enzyme 1α

698	IRGM	Immunity-related GTPase family M protein
699	LC3	MAP1LC3B
700	mTORC1	Mechanistic target of rapamycin
701	MOI	Multiplicity of infection
702	NOD2	Nucleotide-binding oligomerisation domain-containing protein 2
703	PBMC	Peripheral blood mononuclear cells
704	PDI	Protein disulphide isomerase
705	PERK	Protein kinase R (PKR)-like endoplasmic reticulum kinase
706	PFA	Paraformaldehyde
707	PMA	Phorbol myristate acetate
708	RAC1	Ras-related C3 botulinum toxin substrate 1
709	p-rpS6	Phosphorylated ribosomal protein S6
710	TNF-α	Tumour necrosis factor alpha
711	UC	Ulcerative colitis
712	UPR	Unfolded protein response
713	XBP1	x-box-binding protein 1

714

715 # Table 1. Pediatric patient genotype

716 *CD* Crohn's disease, *UC* Ulcerative colitis, *IBDU* IBD unclassified. *ATG16L1 T300A* genotype:
717 rs2241880. **NOD2* genotype SNPs: *L1007fs* (rs2241880), *G908R* (rs2066845) and *R702W*
718 (rs2066844).

	Non-IBD	**CD**	**UC**	**IBDU**
Cohort (n=29)	9	12	7	1
Genotype *ATG16L1 T300A* (n=26)				
Wildtype	1	2	1	N/A
Heterozygous risk	3	6	3	N/A
Homozygous risk	3	4	3	N/A
Genotype *NOD2 L1007fs* (n=27)				
Wildtype	8	12	7	N/A
Heterozygous risk	0	0	0	N/A
Homozygous risk	0	0	0	N/A
Genotype *NOD2 G908R* (n=27)				
Wildtype	8	11	7	N/A
Heterozygous risk	0	0	0	N/A
Homozygous risk	0	1	0	N/A
Genotype *NOD2 R702W* (n=27)				
Wildtype	7	11	6	N/A
Heterozygous risk	0	1	0	N/A
Homozygous risk	1	0	1	N/A

719

Figure Legends

Figure 1: Modulation of autophagy by current IBD drugs

HEK293 GFP-LC3 cells were untreated (i) or treated with DMSO (ii), EBSS (iii), 120μM Azathioprine (iv and x), 100μg/ml Infliximab (v and xi), 120μM Methotrexate (vi and xii), 100μM methylprednisolone (vii and xiii) or 150μM sulfasalazine (viii and xiv) and assessed by live-cell confocal microscopy up to 12hr. 50 cells counted from 3 fields of view and percentage cells with >5 GFP-LC3 puncta quantified (+/- SEM) for all time-points (x-xiv) with 6hr time-point highlighted **p <0.01; ****p < 0.0001 (ix).

Figure 2: Azathioprine activates the autophagy pathway

A) HEK293 GFP-LC3 cells were treated for 6hr with 160nM BafA1 only or BafA1 plus EBSS (i), BafA1 plus 120μM azathioprine (ii) or BafA1 plus 100μg/ml Infliximab (iii). Geometric mean of GFP-LC3-II intensity was assessed by flow cytometry. Fold-change in GFP-LC3-II geometric mean from BafA1 only was quantified (+/-SEM) (iv).

B) HEK293 cells were transfected with GFP-RFP-LC3 plasmid and left untreated (i, v, ix) or treated with 160nM BafA1 (ii, vi, x), EBSS (iii, vii, xi), or 120μM azathioprine (iv, viii, xii) for 6hr, and imaged by confocal microscopy. Percentage of transfected cells exhibiting >10 LC3 puncta was quantified (+/-SEM) (n=5) (xiii) *p <0.05. Number of (RFP+GFP+) and (RFP+GFP-) LC3 puncta were quantified (+/-SEM) (n=5) (xiv) **p <0.01, ***p <0.001.

Figure 3: Azathioprine induces autophagosome accumulation independent of apoptosis

A) THP-1-derived macrophages were untreated (i), or treated with DMSO (ii), EBSS (iii), or 120μM azathioprine (iv) for 6hr. Cells were then immunostained for endogenous LC3 and imaged by confocal microscopy. 30 cells were counted from 3 fields of view and percentage cells with >5 GFP-LC3 puncta quantified (+/- SEM) *p <0.05; **p < 0.01 (v).

B) THP-1-derived macrophages were left untreated (i, v) or treated with DMSO (ii, vi), 120μM azathioprine (iii, vii) or 30μM camptothecin (iv, viii) for 6hr (i-iv) and 24hr (v-vii). Cells were stained with Annexin-V/PI and analysed by flow cytometry. Mean percentage population in each quadrant was quantified (+/- SEM) **p value <0.01, ***p value <0.001, ****p value <0.0001 (ix) compared to untreated for corresponding time-point and quadrant.

Figure 4: Azathioprine stimulates the UPR

THP-1-derived macrophages were left untreated, or treated with DMSO, 60μM or 120μM azathioprine, or EBSS for 2, 4, 6, 16 and 24hr. Expression of PERK was determined by RT-qPCR and is displayed in Log_{10} scale (i). 6hr time-point, including treatment with 0.5μg/ml Brefeldin A quantification (+/- SEM) is shown for PERK (ii), ATF4 (iii), CHOP (iv), PDI (vi) and BiP (vii). Using 2^{-ddct}: *p <0.05, **p <0.01, ****p <0.0001.

Figure 5: Azathioprine modulates autophagy via mechanisms involving mTORC1 and PERK.

A) THP-1-derived macrophages were left untreated or treated with DMSO, azathioprine (60-120μM), EBSS or the mTORC1 inhibitor rapamycin (100nM) for 6hr. Protein lysates were immunoblotted for rpS6, phosphorylated rpS6 (p-rpS6 (S235/236)) and actin (i). rpS6/p-rpS6 density normalized to actin was quantified as a percentage of untreated (ii). Representative blot from n=3.

B) THP-1-derived macrophages were left untreated, or treated with DMSO, 120μM azathioprine, EBSS, or 0.5μg/ml Brefeldin A for 6hr in the absence or presence of PERK inhibitor. Protein lysates were immunoblotted for rpS6, phosphorylated rpS6 (p-rpS6 (S235/236)), phosphorylated eIF2α (p-eIF2α (S51) and tubulin (i). rpS6/p-rpS6 density (ii) and p-eIF2α density (iii) normalized to tubulin was quantified. Representative blot from n=3.

C) THP-1-derived macrophages were left untreated, or treated with 120μM azathioprine, or EBSS for 6 hr in the absence (i-iii) and presence (iv-vi) of PERK inhibitor and immunostained for LC3. 100 cells were counted per treatment and percentage cells with >5 GFP-LC3 puncta quantified (+/- SEM) *p <0.05 (vii).

Figure 6: Azathioprine enhances clearance of intracellular AIEC and dampens the inflammatory response.

A) THP-1-derived macrophages were infected with AIEC and gentamicin protection assay performed in the absence or presence of DMSO or 120μM azathioprine. CFU/ml of cell lysates were enumerated, and fold-change mean CFU/ml from untreated was calculated (+/- SEM), **p <0.01.

B and C) THP-1-derived macrophages were infected with AIEC-mCherry and gentamicin protection assay performed in the absence or presence of DMSO or 120μM azathioprine. Fluorescent AIEC were enumerated and percentage cells with intracellular bacteria quantified (+/- SEM), *p <0.05, **p <0.01, ***p <0.001.

D) THP-1-derived macrophages were infected with AIEC (i) or treated with 200ng/ml LPS (ii) and left untreated or treated with DMSO or 120μM azathioprine for 6hr. Expression of TNF-α

781 was normalized to untreated and mean fold-change expression quantified from n=3 (+/- SEM)
782 (i-ii). Using 2^{-ddct} : *p <0.05.

783 **Figure 7: Azathioprine activates autophagy in PBMC and monocytes from pediatric patients.**

784 PBMC isolated from non-IBD control and IBD patients were left untreated or treated with
785 120µM azathioprine for 6hr. PBMC were stained with surface markers for classification into
786 populations and for endogenous LC3-II. Geometric mean of LC3-II intensity was quantified by
787 flow cytometry and mean of LC3-II geometric mean (+/-SEM) is shown for total PBMC (I, iii)
788 and total monocytes (ii) for each non-IBD and IBD patient group (i-ii) and each *ATG16L1*
789 genotype (iii**)**. One-way ANOVA with Tukey's multiple comparison was used to compare LC3-
790 II geometric mean between patient groups in untreated cells. Within each patient group
791 paired, two tailed t test was used to compare LC3-II geometric mean of untreated and
792 azathioprine-treated cells. *p < 0.05, **p <0.01.

793 **Table S1: Concentration and manufacturer details of reagents used for cell treatments.**

794 Working concentrations were diluted in appropriate growth media.

795 **Table S2: Antibody details**

796 *WB* western blot, *IF* immunofluorescent staining, *F* flow cytometry, *IHC*
797 immunohistochemistry. All primary and secondary antibodies were prepared in 1% FBS or
798 goat serum.

799 **Table S3: qPCR Primer Details**

800 *FW* forward and *RV* reverse primer sequences.

801 **Table S4: Pediatric patient demographics**

CD Crohn's disease, *UC* Ulcerative colitis, *IBDU* IBD unclassified. *SD* Standard deviation. *Non-IBD diagnosis included normal (4 patients), mild constipation (1 patient), Irritable Bowel Syndrome (IBS) (3 patients) and threadworms (1 patient). [a]Paris Classification for CD: *L1* ileal, *L2* colonic, *L3* ileocolonic, *L4a* upper disease proximal to ligament of Treitz; *B1* non-stricturing and non-penetrating, *B2* stricturing, *B3* penetrating, *p* perianal disease modifier [72]. [b]Paris Classification for UC: *E1* ulcerative proctitis, *E2* left-sided UC (distal to splenic flexure), *E3* extensive (hepatic flexure distally), *E4* pancolitis (proximal to hepatic flexure); *S0* never severe, *S1* ever severe as defined by Pediatric Ulcerative Colitis Activity Index (PUCAI) [72]. *5-ASA* 5-aminosalisylates.

Figure S1: GFP-LC3 Flow Cytometry in HEK293 GFP-LC3 cells.

Schematic diagram showing cell permeabilization with 0.05% saponin to remove cytosolic GFP-LC3 to allow flow cytometery analysis [23] (i). HEK293 GFP-LC3 cells were either untreated or treated with 160nM bafilomycin for 6 hours. Cells were washed without (ii) or with (iii) cell permeabilization with 0.05% saponin to remove cytosolic GFP-LC3 before fixation. Geometric mean of GFP-LC3 fluorescent intensity of cells was quantified by flow cytometry and analysed using FlowJo software (ii-iii).

Figure S2: Differentially Expressed Genes from RT^2 Profiler™ PCR Array for Human Autophagy Genes when treated with Azathioprine

THP-1-derived macrophages were untreated or treated with 120µM azathioprine for 6 hours. mRNA was extracted and converted to cDNA for RT-qPCR analysis using the RT^2 Profiler™ PCR Array for Human Autophagy genes according to manufacturer instructions. The calibrating sample was untreated cells and relative expression for azathioprine treatment is displayed as fold-change, with upregulated genes calculated as 2^{-ddCT} and downregulated genes as 2^{ddCT}. Differentially expressed genes are shown, with 1.5-fold change in expression considered as the threshold for differential expression.

Figure S3: Effect of azathioprine on growth of AIEC, clearance of intracellular AIEC and pro-inflammatory cytokine responses

LB broth was inoculated from an overnight culture of AIEC to an optical density of 0.05 at 600nm. The cultures were untreated, or treated with DMSO, or 120µM of azathioprine and incubated at 37^{o}C with shaking at 200RPM. Optical density at 600nm was measured every 0.5 hours and plotted in logarithmic scale to show growth phases.

Figure S4: Azathioprine activates autophagy in monocyte subsets, T cells, B cells and NK cells from pediatric patients.

PBMC isolated from non-IBD control and IBD patients were left untreated or treated with 120µM azathioprine for 6h. PBMC were stained with surface markers for classification into populations and for endogenous LC3-II. Geometric mean of LC3-II intensity was quantified by flow cytometry and mean of LC3-II geometric mean (+/-SEM) is shown for classical monocytes (i), intermediate monocytes (ii), non-classical monocytes (iii), T cells (iv), B cells (v) and NK cells (vi) for each non-IBD and IBD patient group. One-way ANOVA with Tukey's multiple comparison was used to compare LC3-II geometric mean between patient groups in untreated cells. Within each patient group paired, two tailed t test was used to compare LC3-II geometric mean of untreated and azathioprine-treated cells. *$p < 0.05$, **$p < 0.01$.

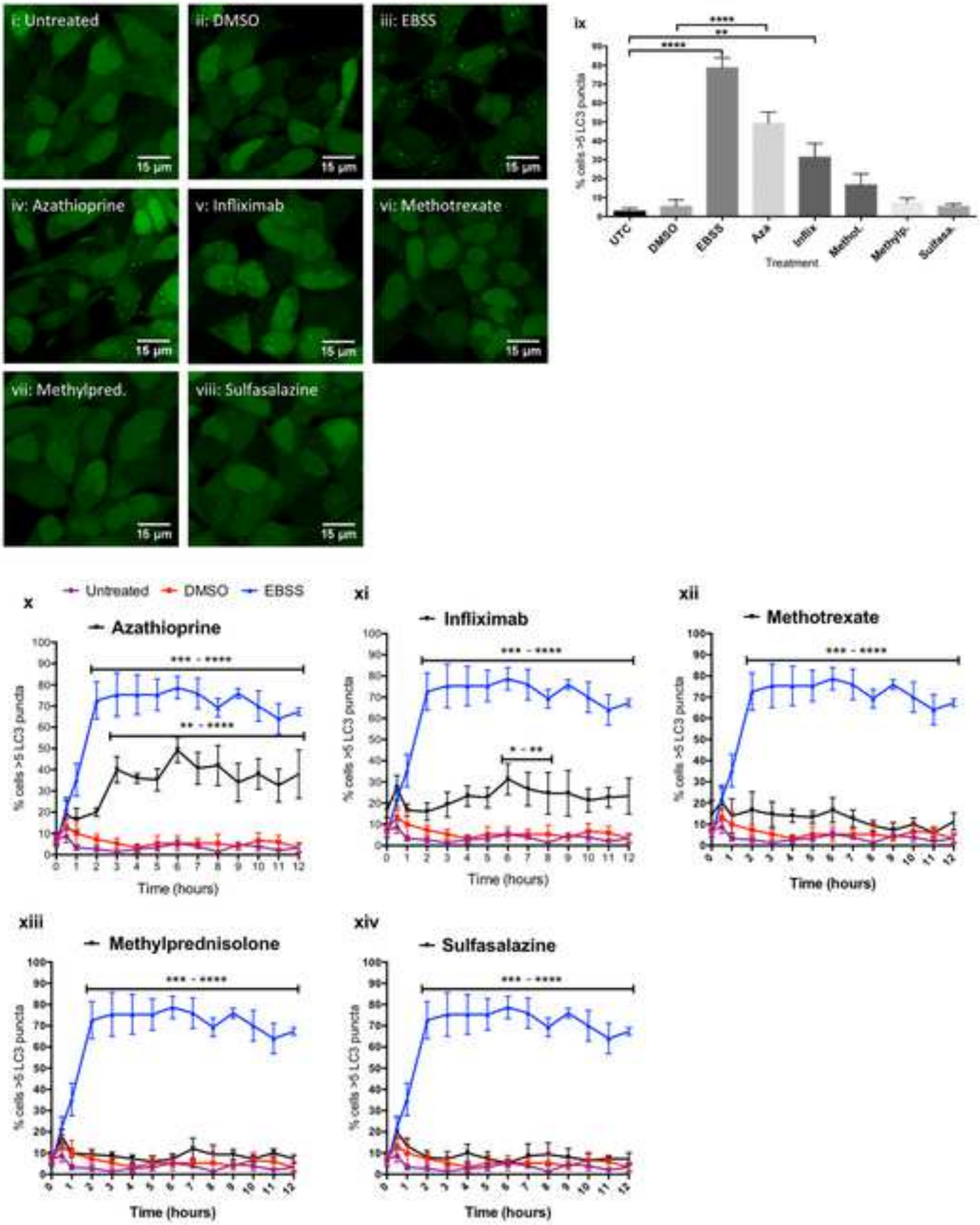

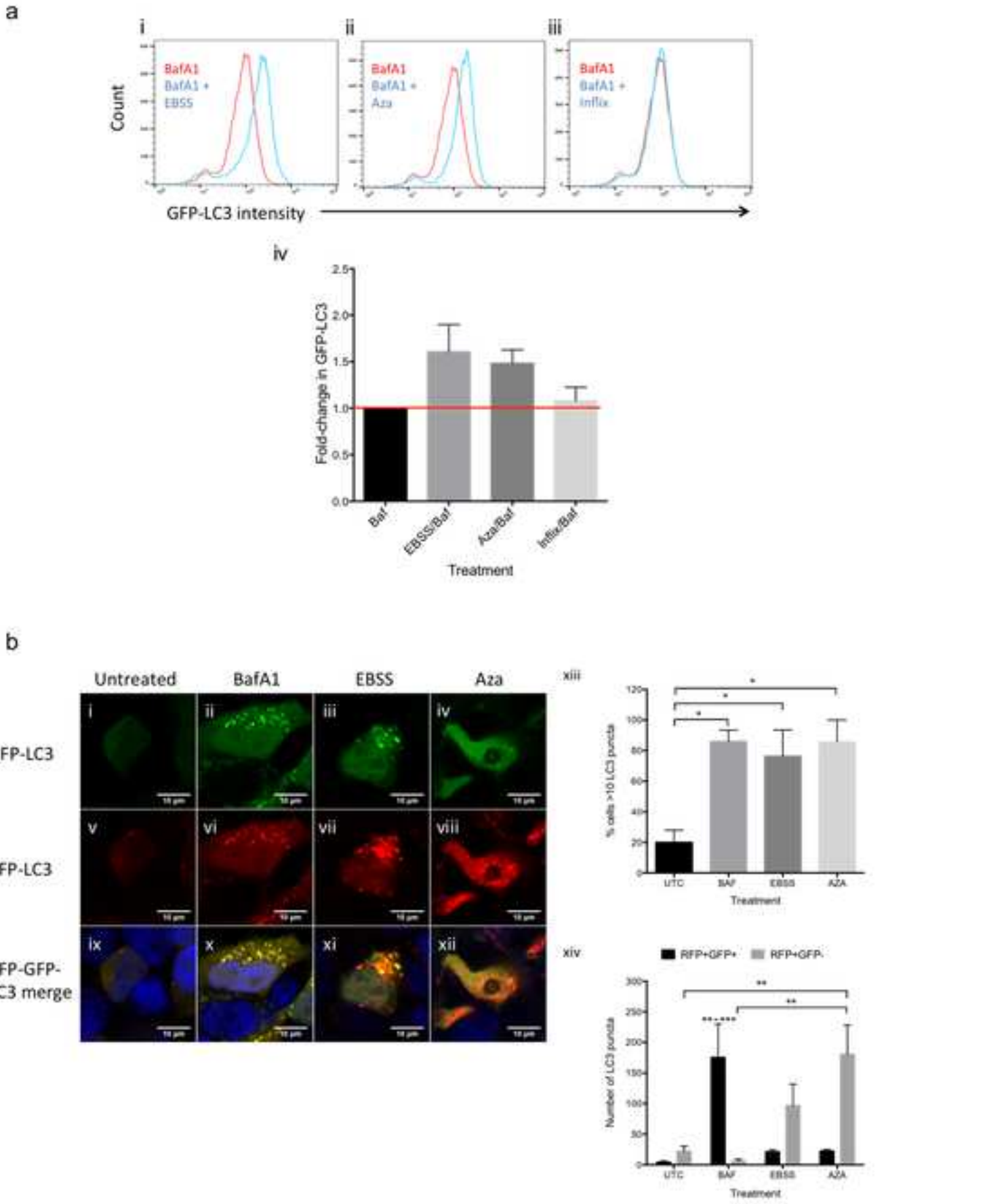

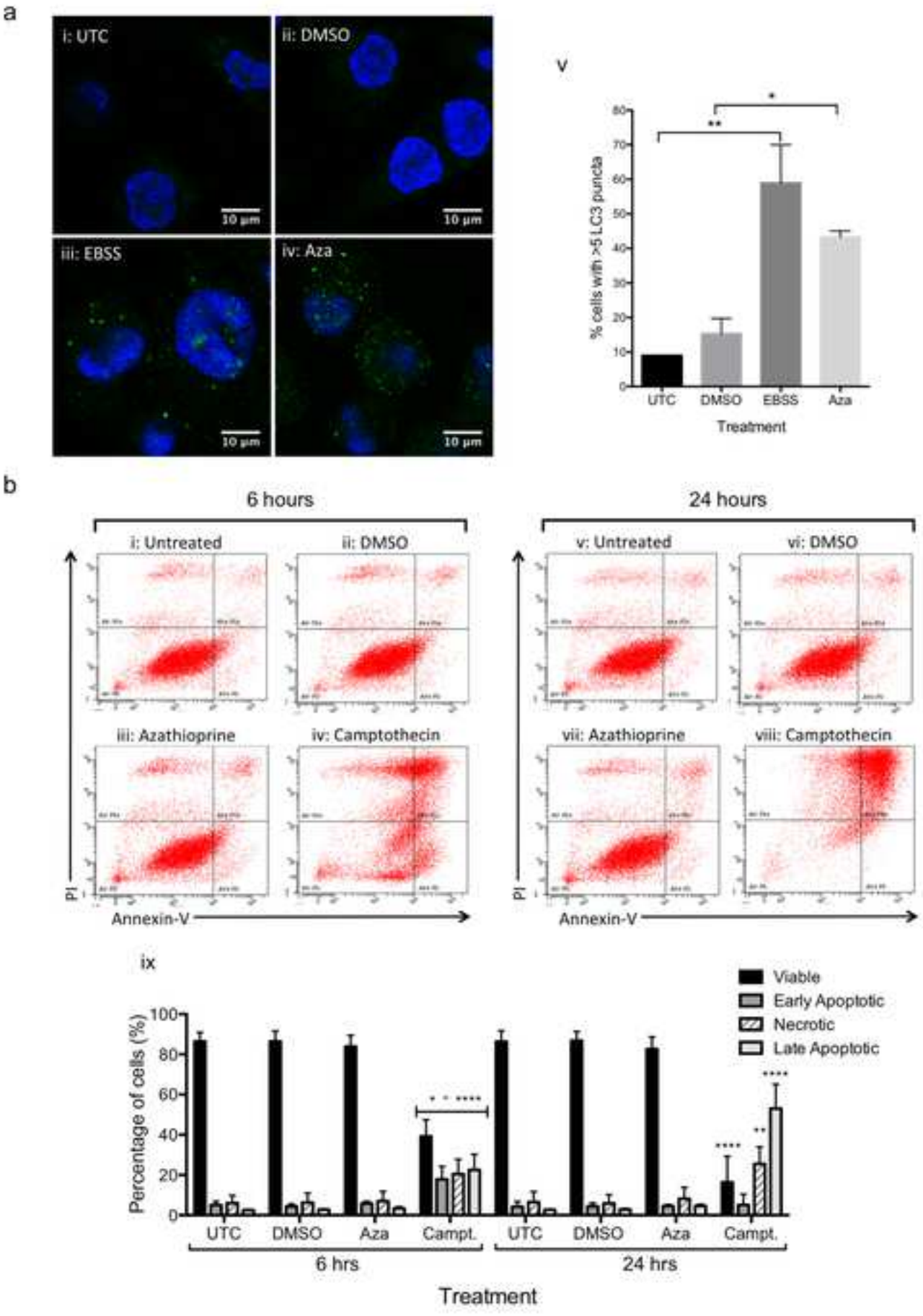

Fig 4

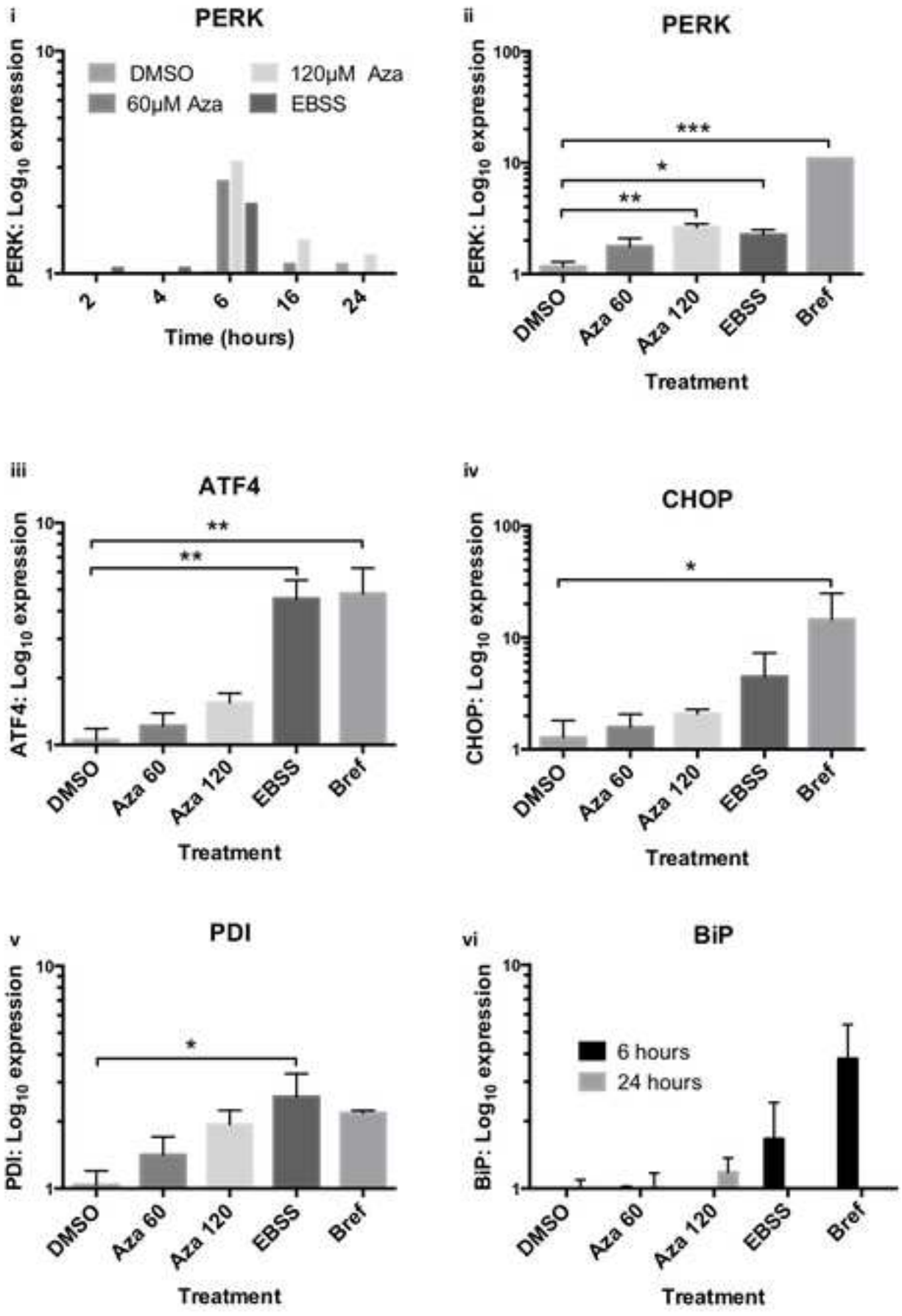

Fig 5

Click here to access/download;Image;Fig 5.tiff

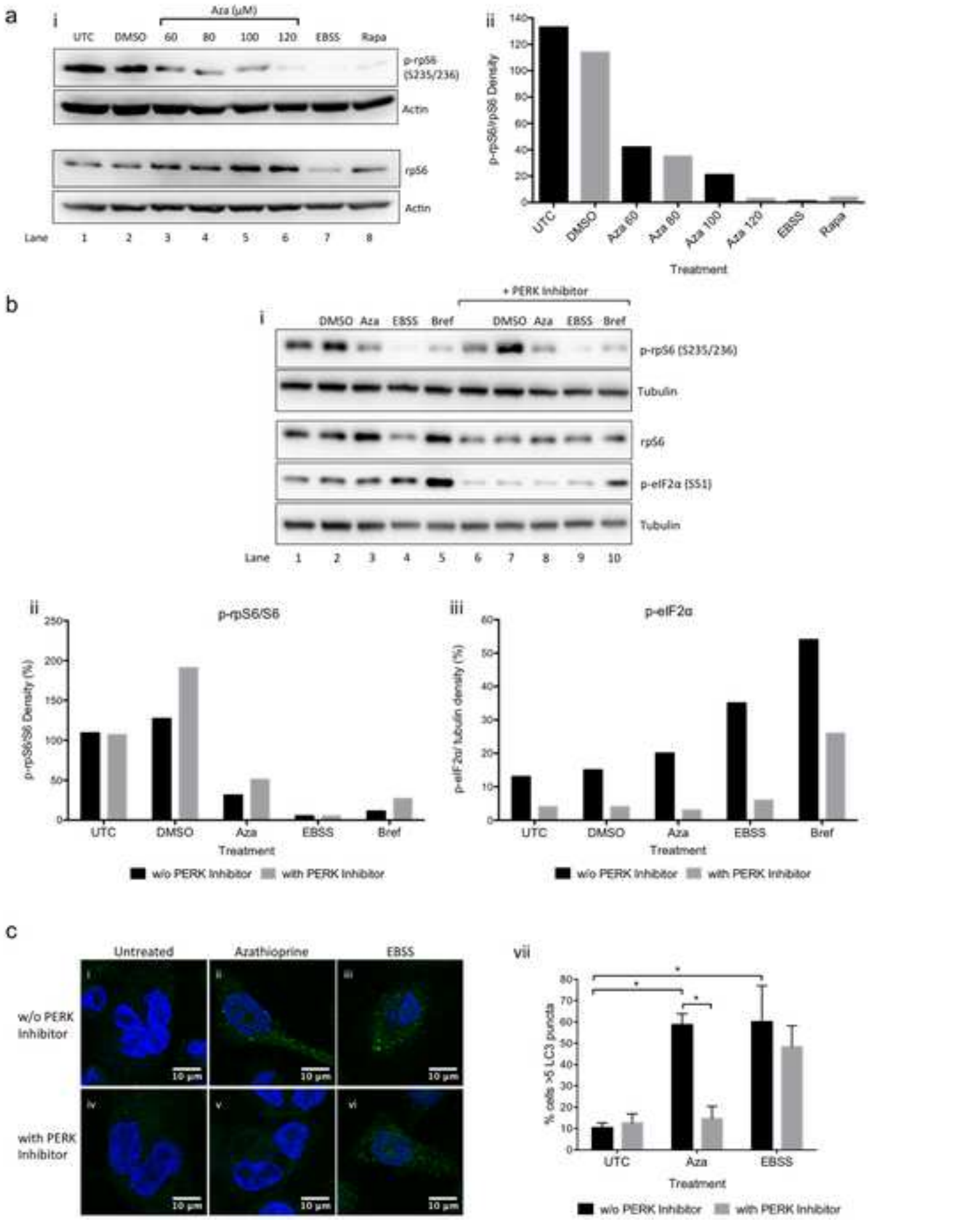

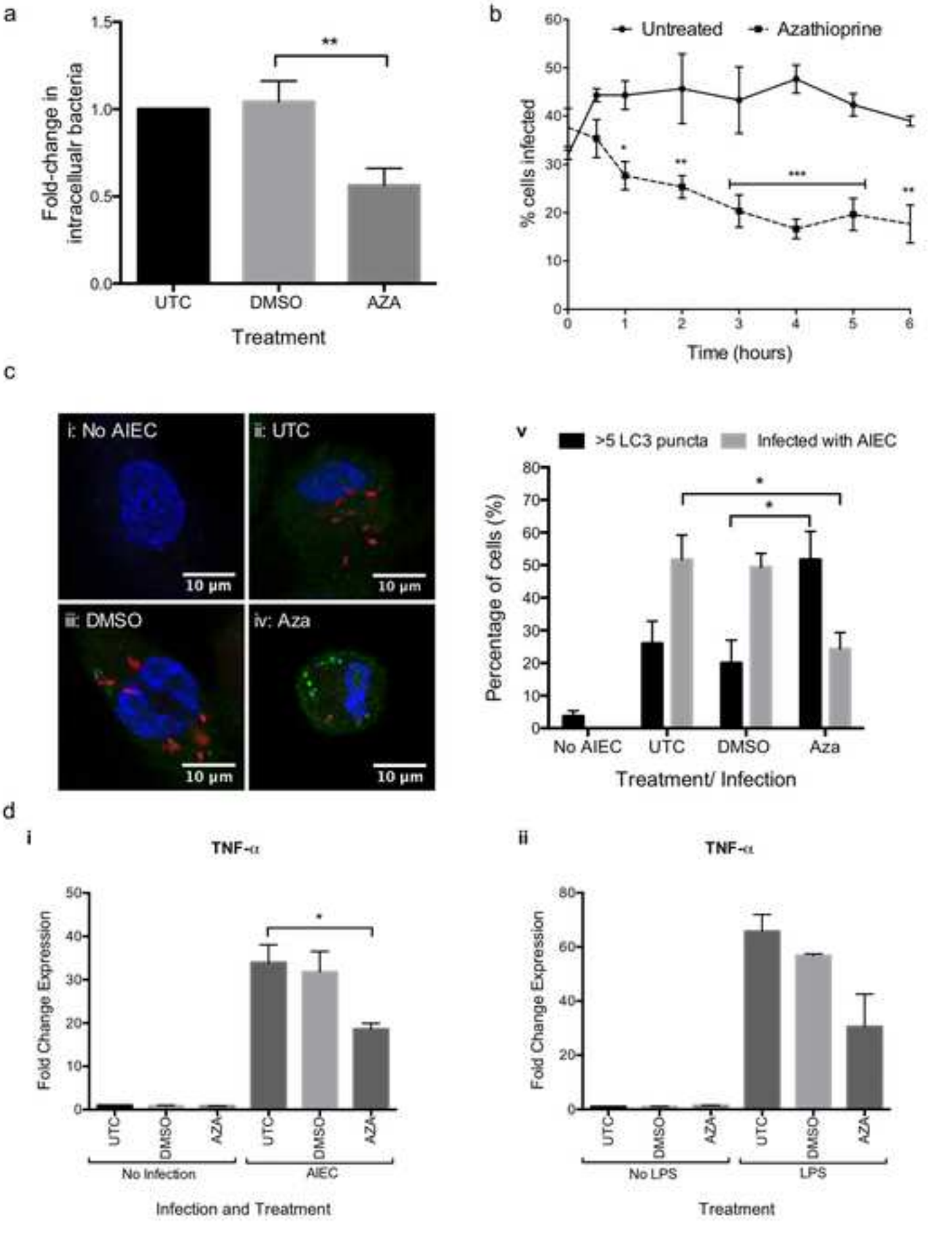

Fig 7

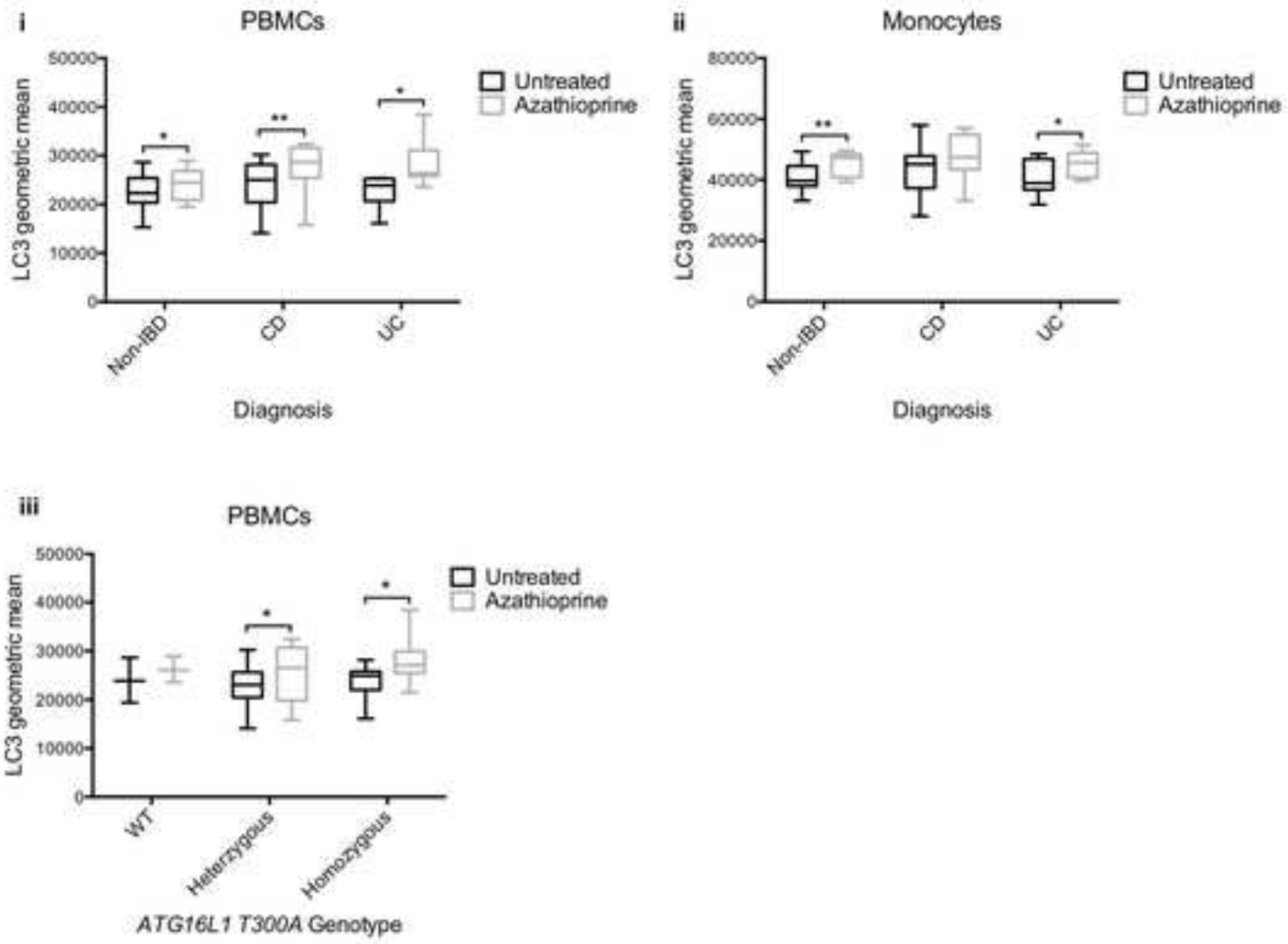

Reagents	Stock conc.	Working conc.	Manufacturer
Azathioprine, 6-mercaptopurine, methotrexate, methylprednisolone, sulfasalazine	400mM in DMSO	1-150µM	Tocris, Abingdon, UK
Bafilomycin A1	1mg/ml in DMSO	160nM	Santa Cruz Biotechnology, Dallas, Texas, USA
Brefeldin A from *Penicillium brefeldianum*	10mg/ml in DMSO	0.5µg/ml	Sigma-Aldirch, Irvine, UK
PERK inhibitor I (GSK2606414)	5µM in DMSO	50nM	Calbiochem®, Merck Millipore, Watford, UK
Rapamycin	2mg/ml	100nM	Sigma, Life Sciences, UK
Remicade® (infliximab)	10mg/ml in dH_2O	5-100µg/ml	A gift from David Hoole, RHSC

Type	Antibody	Clone (Isotype)	Use (Conc.)	Manufacturer
Primary Antibodies	Ms actin	ACTN05 [C4]	WB (1 in 5000)	Abcam, Cambridge, UK
	Rb phospho-eIF2α (S51)	119A11	WB (1 in 1000)	Cell Signalling, Hitchin, UK
	Ms LC3	2G6	WB 1 in 1000)	NanoTools Teningen, Germany
	Rb LC3	PM036	IF, IHC (1 in 1000)	MBL Intl., MA, USA
	Rb cleaved-PARP	D214	WB (1in 1000)	Cell Signalling
	Ms rpS6	54D2	WB (1 in 1000)	Cell Signalling
	Rb phospho-rpS6 (S235/236)	2F9	WB (1 in 1000)	Cell Signalling
	Rb Tubulin	GR187587-1	WB (1 in 5000)	Abcam
PBMC surface markers	PE-Cy™7 Ms Anti-Human CD3	UCHT1 (MOPC-21)	F (1 in 40)	BD Pharmingen™, Oxford, UK
	PE-Ms Anti-Human CD14	M5E2	F (1 in 10)	BD Pharmingen™
	PerCP-Cy™5.5 Ms Anti-Human CD16	3G8	F (1 in 40)	BD Pharmingen™
	BV786 Ms Anti-Human CD19	HIB19 (X40)	F (1 in 40)	BD Horizon™, Oxford, UK
	BV650 Ms Anti-Human CD56	NCAM16.2 (27-35)	F (1 in 40)	BD Horizon™
	BV421 Ms Anti-Human HLA-DR	G46-6 (Polyclonal)	F (1 in 40)	BD Horizon™
Secondary Antibodies	Goat anti-Rb and goat anti-Ms IgG/HRP	F:1.0 and F:1.5	WB (1 in 5000)	Dako, Glostrup, Denmark
	Goat anti-Rb IgG-FITC		IF (1 in 1000), F (1 in 500)	Sigma

Target Gene	FW Primer	RV Primer	Manufacturer
Actin	GGACTTCGAGCAAGAGATGG	AGGAAGGAAGGCTGGAAGAG	Eurofins Genomics, Ebersberg, Germany
ATF4	CTCCGGGACAGATTGGATGTT	GGCTGCTTATTAGTCTCCTGGAC	Eurofins Genomics
BiP (GRP78)	TATGGTGCTGCTGTCCAGG	CTGAGACTTCTTGGTAGGCAC	Eurofins Genomics
CHOP	AGCTGGAAGCCTGGTATGAGG	GTGCTTGTGACCTCTGCTGG	Eurofins Genomics
PERK	GGAAACGAGAGCAGGATTTATT	ACTATGTCCATTATGGCAGCTTC	Eurofins Genomics
PDI	TGCCCAAGAGTGTGTCTGAC	CTGGTTGTCGGTGTGGTC	Eurofins Genomics
RPL13A	Primer Mix	Primer Mix	PrimerDesign Ltd, Chandler´s Ford, UK
TNFα	GCTGCACTTTGGAGTGATCG	GCTTGAGGGTTTGCTACAACA	Eurofins Genomics

Table S4

	Non-IBD*	CD	UC	IBDU
Cohort (n=29)	9	12	7	1
Age years (mean +/- SD)	10.7 +/- 3.3	12.8 +/- 2.7	13.4 +/- 2.5	9.7 +/- 0
Disease duration: years (mean +/- SD)	N/A	1.4 +/- 2.3	1.9 +/- 3.4	0
Gender				
Male	6	11	3	0
Female	3	1	4	1
Disease Location				
L1[a] E1[b]	N/A	1[a]	0[b]	0[b]
L2[a] E2[b]	N/A	1[a]	3[b]	1[b]
L3[a] E3[b]	N/A	2[a]	1[b]	0[b]
L1/L4a[a] E4[b]	N/A	1[a]	3[b]	0[b]
L2/L4a[a]	N/A	1[a]	N/A	N/A
L3/L4a[a]	N/A	5[a]	N/A	N/A
Disease Behaviour [a]				
B1[a] S0[b]	N/A	8[a]	5[b]	1[b]
B2[a] S1[b]	N/A	1[a]	2[b]	0[b]
B3[a]	N/A	0[a]	N/A	N/A
B1p[a]	N/A	2[a]	N/A	N/A
Therapy (n)				
None	N/A	7	4	1
Immunosuppressants	N/A	1	0	0
Biologics	N/A	3	0	0
Biologics, thiopurines	N/A	1	0	0
Biologics, 5-ASA	N/A	0	1	0
5-ASA, thiopurines	N/A	0	2	0

Fig S1

Click here to access/download;Supplementary Material For Review;Fig S1.tiff

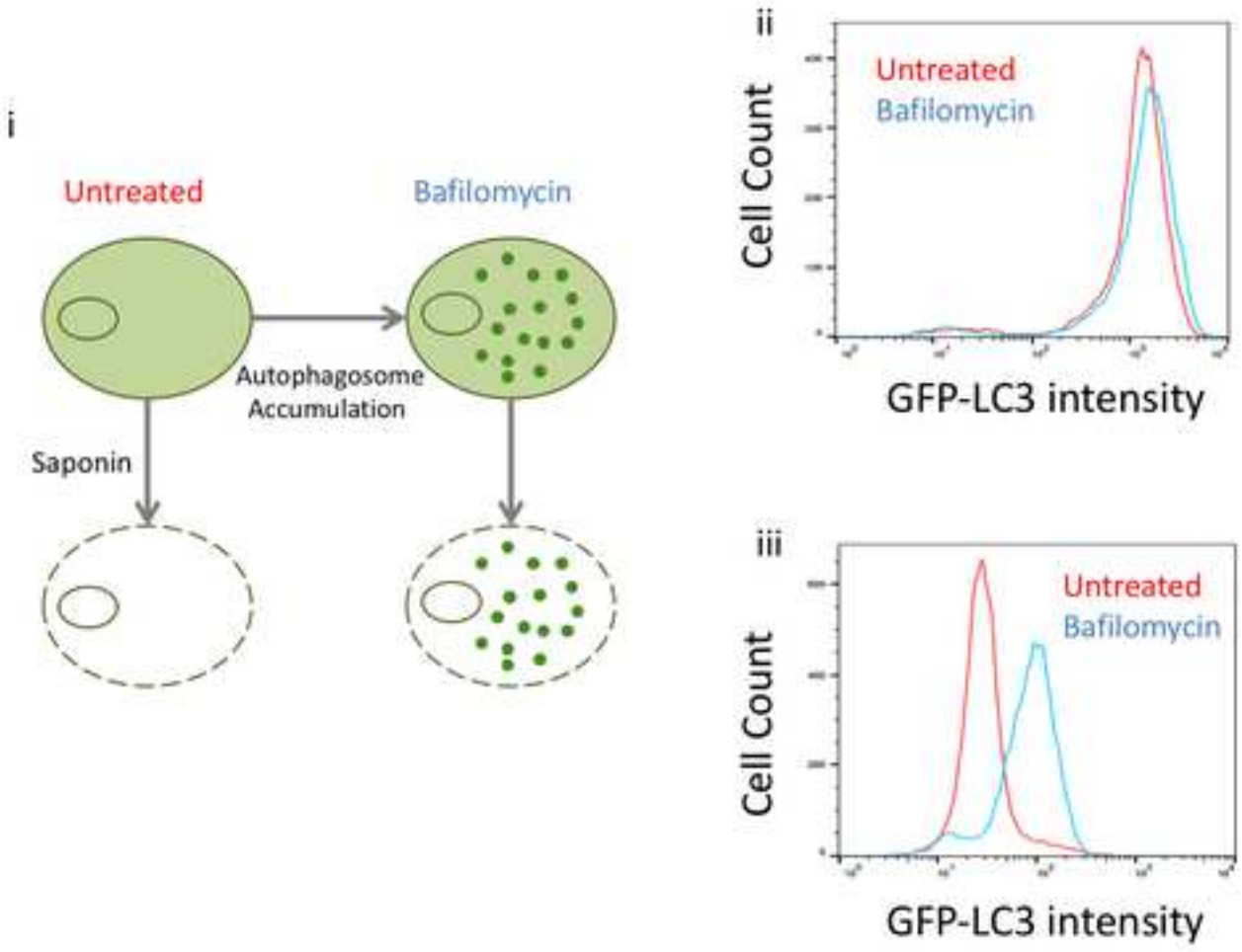

Fig S2

Click here to access/download;Supplementary Material For Review;Fig S2.tiff

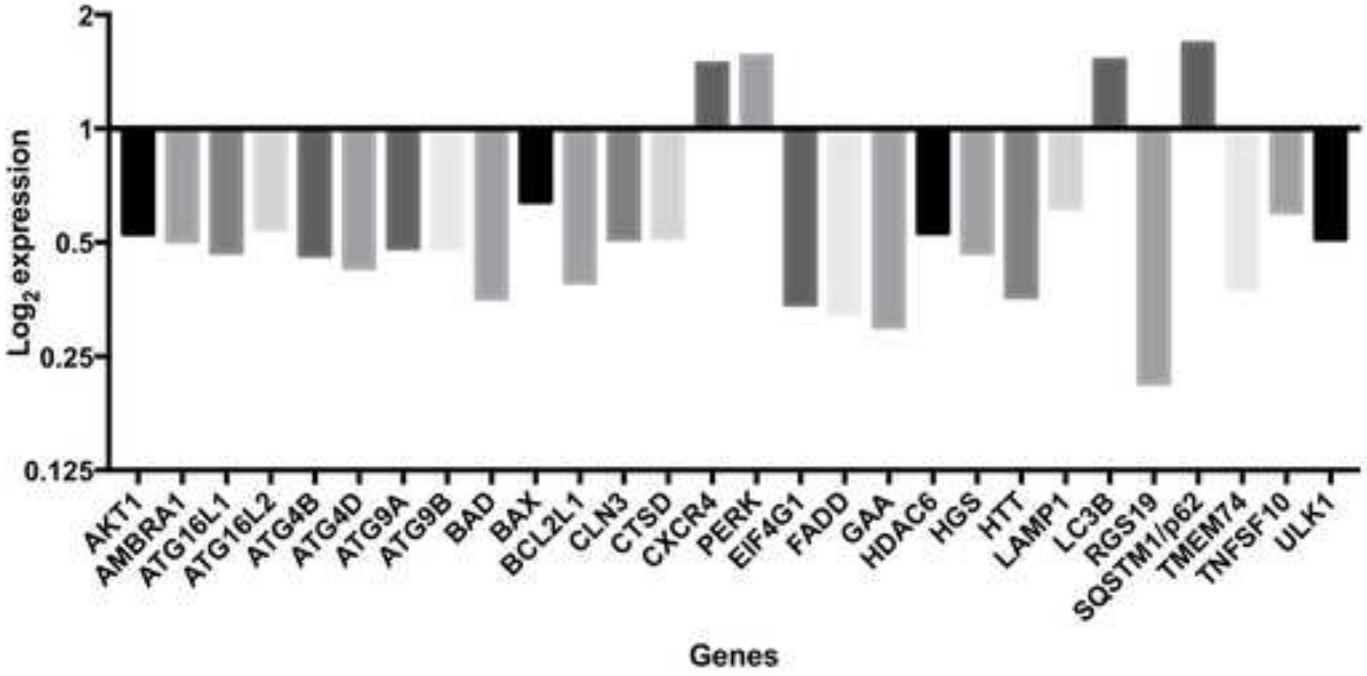

Fig S3

Click here to access/download;Supplementary Material For Review;Fig S3.tiff

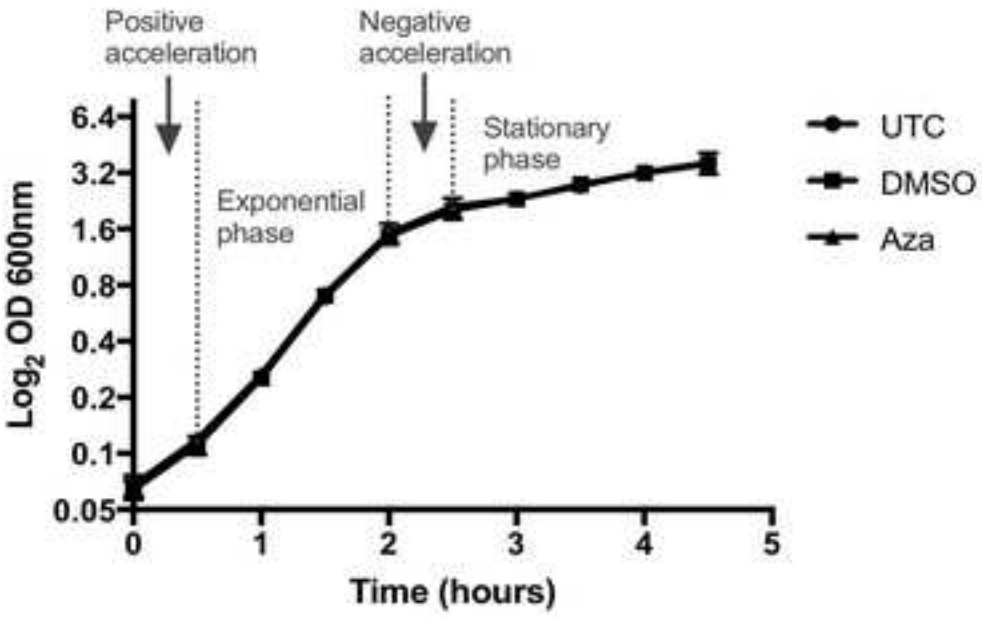

Fig S4

Click here to access/download;Supplementary Material For Review;Fig S4.tiff